AN ANALYSIS OF SOLAR RADIO BURST TYPES III AND IV WITH RELATION TO SOLAR ACTIVITIES AND GEOMAGNETIC STORM

NABILAH BINTI RAMLI

FACULTY OF SCIENCE
UNIVERSITY OF MALAYA
KUALA LUMPUR

2018

AN ANALYSIS OF SOLAR RADIO BURST TYPES III AND IV WITH RELATION TO SOLAR ACTIVITIES AND GEOMAGNETIC STORM

NABILAH BINTI RAMLI

DISSERTATION SUBMITTED IN FULFILMENT OF THE REQUIREMENTS FOR THE DEGREE OF MASTER OF SCIENCE

DEPARTMENT OF PHYSICS
FACULTY OF SCIENCE
UNIVERSITY OF MALAYA
KUALA LUMPUR

2018

UNIVERSITY OF MALAYA

ORIGINAL LITERARY WORK DECLARATION

Name of Candidate: **NABILAH BINTI RAMLI**

Matric No: **SGR 130088**

Name of Degree: **MASTER OF SCIENCE**

Title of Project Paper/Research Report/Dissertation/Thesis ("this Work"):

"AN ANALYSIS OF SOLAR RADIO BURST TYPES III AND IV WITH RELATION TO SOLAR ACTIVITIES AND GEOMAGNETIC STORM"

Field of Study: **EXPERIMENTAL PHYSICS**

I do solemnly and sincerely declare that:

(1) I am the sole author/writer of this Work;
(2) This Work is original;
(3) Any use of any work in which copyright exists was done by way of fair dealing and for permitted purposes and any excerpt or extract from, or reference to or reproduction of any copyright work has been disclosed expressly and sufficiently and the title of the Work and its authorship have been acknowledged in this Work;
(4) I do not have any actual knowledge nor do I ought reasonably to know that the making of this work constitutes an infringement of any copyright work;
(5) I hereby assign all and every rights in the copyright to this Work to the University of Malaya ("UM"), who henceforth shall be owner of the copyright in this Work and that any reproduction or use in any form or by any means whatsoever is prohibited without the written consent of UM having been first had and obtained;
(6) I am fully aware that if in the course of making this Work I have infringed any copyright whether intentionally or otherwise, I may be subject to legal action or any other action as may be determined by UM.

Candidate's Signature Date:

Subscribed and solemnly declared before,

Witness's Signature Date:

Name:

Designation:

AN ANALYSIS OF SOLAR RADIO BURST TYPES III AND IV WITH RELATION TO SOLAR ACTIVITIES AND GEOMAGNETIC STORM

ABSTRACT

Solar activities are natural phenomena that occur at the solar surface by ejecting energy into interplanetary space and consequently hitting Earth's atmosphere where the commencement of geomagnetic storms. Generally, solar radio bursts originated at the same level as the solar flares, Coronal Mass Ejections (CMEs) and shock at solar atmosphere which the Sun project the radio energy into the interstellar medium. This is a novel study to investigate the correlation between solar burst type IV and type III based on their properties. The analysis is based on the statistical data of type IV and type III solar bursts from 2006 – 2011 and 10 selected events over 2006-2015. The statistics of solar burst type IV associated with type III were obtained through e-Callisto (Compact Astronomical Low-frequency Low-cost Instrument for Spectroscopy Transportable Observatory) Spectrometer in the years 2006 until 2011. The point of this examination is to discover whether type III bursts preserved energy to solar bursts type IV thus led to the formation of geomagnetic storm. Statistical data from this study showed that most of the burst type IV were preceded and followed by type III burst. The total number of type IV events studied was 37, with 20 preceded by type III and the remainder with other type. Predominantly, solar bursts events are accompanied with great solar flares (class X and M) producing major storms. Although the study did not show much correlation between bursts type IV and type III in producing these storms, there are several possible explanations from this result. It may be the case that solar events such as solar flare, CMEs and active region ejected from the solar disc is not heading towards Earth and the energy has eventually disperses into the interplanetary medium.

Keywords: Solar radio burst, Solar wind, Solar flare, CME and Geomagnetic storm.

ANALISIS LETUSAN RADIO SURIA JENIS III DAN IV DENGAN HUBUNGANNYA KE ATAS AKTIVITI SURIA DAN RIBUT GEOMAGNETIK

ABSTRAK

Aktiviti suria adalah fenomena semula jadi yang berlaku pada permukaan Matahari dengan menghamburkan tenaga ke dalam ruang antara planet dan seterusnya meghentam atmosfera Bumi di mana bermulanya ribut geomagnetik. Umumnya, letusan radio suria berasal pada paras yang sama sebagaimana suar suria, Ledakan Jisim Korona (LJK) dan kejutan di atmosfera suria dimana Matahari menghalakan tenaga radio ke dalam medium antara bintang. Ini merupakan satu kajian baru untuk menyiasat hubungan antara letusan suria jenis IV dan jenis III berdasarkan sifat-sifat mereka. Kajian dijalankan berdasarkan statistik jenis IV and jenis III letusan suria dari tahun 2006-2011 dan 10 peristiwa yang telah dipilih dari 2006-2015. Statistik letusan suria jenis IV diiringi jenis III telah diperolehi melalui e-Callisto (Kompaun Instrumen Astronomi Frekuensi rendah, Kos rendah untuk Spektroskopi Angkutan Balaicerap) Spektrometer pada tahun 2006 hingga 2011. Tujuan kajian ini adalah untuk mencari samaada letusan jenis III memberi tenaga kepada letusan suria jenis IV sekaligus menyebabkan kepada pembentukan ribut geomagnetik. Data statistik menunjukkan, sebahagian besar letusan jenis IV telah didahului dan diikuti oleh letusan jenis III. Jumlah keseluruhan peristiwa jenis IV dikaji adalah 37, dengan 20 peristiwa didahului dengan jenis III dan selebihnya dengan jenis lain. Kebanyakannya, kesemua peristiwa yang disertakan dengan suar suria yang hebat (kelas X dan M) menghasilkan ribut yang kuat. Walaupun kajian tidak menunjukkan hubungan yang jelas antara letusan jenis IV dan jenis III dengan ribut, terdapat beberapa penjelasan untuk hasil ini. Ini mungkin terjadi disebabkan peristiwa Matahari seperti suar suria, CME dan tompok yang ditolak keluar dari cakera matahari tidak menghala ke Bumi, lalu tenaga tersebar ke dalam medium antara planet.

Kata Kunci: Letusan radio suria, Suar suria, Angin suria, CME & Ribut geomagnetik.

ACKNOWLEDGEMENTS

Alhamdulillah, first and foremost, I would like to thank to Allah, Lord of Universe, The Merciful and The Gracious. I would like to express my gratitude for His Help and Guidance and also give me strength as well as patience to complete my master study entitled "An Analysis of Solar Radio Burst Types III and IV with Relation to Solar Activities and Geomagnetic Storm".

I would like to express my deep gratitude to Associate Professor Dr. Zamri Bin Zainal Abidin and Dr Zety Sharizat Binti Hamidi, my research supervisors, for their patient guidance, enthusiastic encouragement and useful critiques of this research work. My grateful thanks are also extended to Professor Dr Zainol Abidin Bin Ibrahim for all the warm advice and motivation throughout this study. Finally, I wish to thank my families and friends for their support and encouragement throughout my study.

In addition, I was grateful to CALLISTO network, STEREO, LASCO, SDO/AIA, NOAA, TESIS and SWPC for make their data available.

TABLE OF CONTENTS

LIST OF FIGURES

LIST OF TABLES

LIST OF SYMBOLS AND ABBREVIATIONS

f	:	Frequency
f_p	:	Plasma frequency
f_{pe}		electron plasma frequency
k_p	:	Planetary K-index
P_{noise}	:	Power of noise
P_{signal}	:	Power of signal
ACE	:	Advanced Composition Explorer
CALLISTO	:	Compound Astronomical Low cost Low frequency Instrument for Spectroscopy and Transportable Observatory
CME	:	Coronal Mass Ejection
Dst	:	Disturbance Storm-Time
EUV	:	Extreme Ultraviolet
GOES	:	Geostationary Operational Environmental Satellite
GPS	:	Global Positioning System
LASCO	:	Large Angle and Spectrometric Coronagraph
NASA	:	National Aeronautics and Space Administration
NOAA	:	National Oceanic and Atmospheric Administration
SDO	:	Solar Dynamics Observatory
SNR	:	Signal-to-noise ratio
SOHO	:	Solar and Heliospheric Observatory
SWPC	:	Space Weather Prediction Center
UT	:	Universal time
WDC	:	World Data Center
XRT	:	X-Ray Telescope

LIST OF APPENDICES

CHAPTER 1: INTRODUCTION

The primary goal of this study is to investigate solar radio burst type III and type IV and their relation to solar activities. In radio astronomy, solar radio bursts are thoughtful to be a meaningful characteristic of solar activity since they are normally featured to an unexpected increase in speed of the particles from the Sun (Hamidi et al., 2012). One of the main reasons for identifying solar radio burst is because it provides the essential tool for specifying magnetic, thermal and density structures at the time (Bhattacharya et al., 2013). Solar radio burst at low-frequency originate in the same layers of the solar atmosphere in which geo-effective disturbance most likely start. This is the place where solar flares and coronal mass ejections (CME) are accepted to be propelled.

Basically, solar radio burst can be characterized into five types based on their frequency range. This comprises of; noise-storm burst (Type I), slow-drift burst (Type II), fast-drift burst (Type III), broadband continuum emission (Type IV) and continuum emission at meter wavelength (Type V). It is believed that these bursts are generated by beams of fast electrons at levels of the local plasma frequency or its second harmonic. Solar burst type III is the radio signature of the solar flare. It is composed of accelerated electron beams ejected into the corona and interplanetary medium which are characterized by very fast frequency drifts in the dynamic spectra (Thejappa et al., 2012). Another potential use of type III solar radio burst is that they generally have a huge association with solar flare events (Thejappa et al., 2012). Solar radio type IV burst is a broadband semi continuum feature associated with the decay phase of solar flares and constantly identified with the development of sunspot groups (Zucca et al., 2012). It has been well established that type IV bursts have a high probability of being followed by geomagnetic disturbance (Bell, 1963b).

Solar radio bursts are the radio emission of solar flares that highlight its brief dynamic and exquisite characteristic. This study is focused on monitoring solar radio burst that are generally associated with solar flares and originates from all levels of the solar atmosphere between the lowest chromospheres and the highest outer corona with heights of several solar radii. Solar flares and coronal mass ejection (CME) are energetically the most vital transient phenomena of the solar atmosphere (Nindos et al., 2008). A solar flare is sudden large energy release in the magnetic active region which are the most operating manifestation of solar activity. It may show up as a fast lighting up in H alpha, but coincidentally can have manifestations right through the electromagnetic spectrum and capable ejecting the high energy particles and blobs of plasma into the solar wind. CME is a large scale coronal structure ejected from the Sun and propagate into the interplanetary space (Yoon, 1997). The shock waves that give changing to magnetic field resulted from CME release a fast dense plasma flow associated with 90% of large space weather events on Earth (Richardson et al., 2006).

Therefore, the present study explores the influence of solar radio burst type III and the solar radio burst type IV that will lead to the formation of geomagnetic storm. To accomplish this aim, the solar radio burst associated with solar events was compared to a geomagnetic storm. The geomagnetic storm is a temporary disturbance of the Earth's magnetosphere caused by a solar wind shock wave and/or clouds of magnetic field which typically strikes the Earth's magnetic field 24 to 36 hours after the event. Although very strong solar events can result in near-instantaneous geomagnetic effects, the impacts of most events are felt on Earth a couple of days later. The occurrence of geomagnetic storms is well associated with the Earth-directed coronal mass ejections (CMEs) (Rathore, Gupta, & Parashar, 2014). These events cause disruptions to electrical power grids, damage spacecraft systems and disrupt communications and GPS (Schmidt et al., 2013).

The radio spectrometer of the CALLISTO (Compound Astronomical Low-cost Low-frequency Instrument for Spectroscopy and Transportable Observatory) was used in this research for monitoring solar radio burst. The instruments observe automatically, with their data gathered each day through the internet and stored in a dominant database. The 'burst mode' can be triggered from the spectrograph of CALLISTO automatically. The e-CALLISTO system has already proven to be a valuable new tool for monitoring solar activity and space weather research (Hamidi et al., 2016). Additional data from GOES, ACE, SOHO, and TESIS were used for analysis.

1.1 Problem Statement

Many previous studies have been conducted on the relation of solar radio burst types II and IV with geomagnetic storms (Bell, 1963a; H. Cane & Reames, 1988; M. Kundu, 1962; McLean, 1959). However, no attempt was done to explore the potential association of type III solar radio burst with geomagnetic storm. Furthermore, the current pattern solar radio burst occurrence from 2006 until 2011 mostly shows that type III solar radio bursts are always coupled with type IV solar radio burst and associated with geomagnetic storm. Thus, the purpose of this study is to attempt at finding what is the relation between types III and IV solar radio burst up to the commencement of the geomagnetic storm.

1.2 Objectives

This study aims to experimentally investigate the type III and type IV solar radio bursts with relation to solar activities.

The specific objectives of this study are: -

1. To use global e-CALLISTO data to obtain and characterize types III and IV solar radio burst.

2. To relate the occurrence of type III and type IV solar radio burst with geomagnetic storm.
3. To investigate the occurrence sequence of type III and type IV solar radio burst.
4. To study the effect of radio frequency interference (RFI) on solar radio bursts detections.

1.3 Significance of Study

The relationship between type IV solar radio burst being followed by geomagnetic disturbance cannot be denied anymore. Numerous studies have investigated this relation such as (Bell, 1963b; Cane, Erickson, & Prestage, 2002; Fokker, 1963; McLean, 1959; Thompson, 1962). It is imperative to know, whether in the presence of type III solar radio burst before the onset of the type IV solar radio burst, give effect to the commencement of the geomagnetic storm. Additionally, there is a study from (Thompson, 1962) that states the connection between type III solar radio burst and type IV solar radio burst depends on the fact that these two bursts are produced by fast electrons.

It is notable that type IV solar radio burst and type III solar radio burst are constantly joined by solar flares and/or CME. These solar activities cause changes in the magnetic field on the solar surface, which is one of the factors that contributes to the occurrence of space weather. Subsequently, it will affect the Earth's technology due to changes in Earth's magnetosphere. These progressions are known as geomagnetic storms which indicates the level of the storm's impact on the Earth's magnetic field. Therefore, by studying the occurrence and the parameters of these solar radio bursts, valuable information may be obtained from this study regarding the occurrence of the geomagnetic storm. In addition, such information may also be very important and useful for solar monitoring.

1.4 Dissertation Outline of Chapters

CHAPTER 1 presents the overview of this dissertation, including the problem statement, objectives and the significance of the study.

CHAPTER 2 covers a brief introduction to the Sun, solar activities and solar radio bursts. The structure of the Sun was described from the core to the outer atmosphere. An overview of solar activities such as sunspots, solar flares, Coronal Mass Ejection (CME), solar wind and geomagnetic storm. The effect of solar activity to space and ground technology is described. Also included is the classification of solar radio burst types that cover type I to type V solar radio bursts.

CHAPTER 3 covers the literature review about the magnetic reconnection from the sunspot that led to solar activities. Several explanations about the theory of Bremsstrahlung radiation, Langmuir wave and Moreton wave were given. Other than that, it demonstrates of Radio Frequency Interference (RFI) and portray the effect of RFI to radio spectrometer.

CHAPTER 4 describes of the instruments used to collect solar radio burst data. Explanation of the data collection for solar flare, CME and geomagnetic storm were given. The data treatment of solar radio burst was also showed.

CHAPTER 5 presents the statistical results from 2006 until 2011 together with selected events chosen from 2006 – 2015. Included are the data analysis and discussion of the relation between solar burst with the solar activities based on their parameters.

CHAPTER 6 Summarizes the study.

CHAPTER 2: THE SUN AND SOLAR ACTIVITY

2.1 Fundamentals of Sun

The Sun is an enormous star in our solar system with the radius of approximately 700,000 km. It is a major source of energy that powers weather, climate and life on Earth. The glowing ball of gas is held together by its own gravity and powered by nuclear fusion at its center. The physical and chemical properties of size, mass, density, rotation rate, and temperature are familiar with other the planets (Chaisson & McMillan, 2014). Other than that, the Sun is an intense radiator that emits a continuum of electromagnetic radiation from X-ray, ultraviolet, optical, infrared and radio wavelength (Goss, 2013).

To better understanding the structure of the Sun, Figure 2.1 demonstrates the main regions of the Sun from the interior to the outer corona. It starts with the photosphere, the part of the Sun that can be seen. The photosphere is the region at the Sun's surface that emits all the electromagnetic radiation with a radius of around 700,000 km. It is believed, solar activities such as solar flare and sunspot were generated on this layer (Ali et al., 2016).

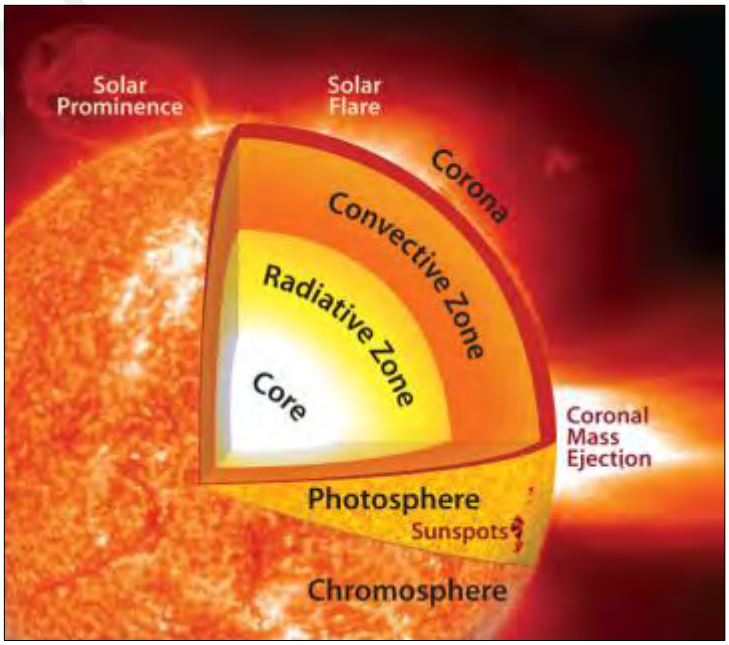

Figure 2.1: The main solar structures.

The next layer is chromosphere. It lies over the photosphere which is the Sun's lower atmosphere with a thickness of around 1500 km. Generally, most of the absorption lines found in the Sun spectrum are originates in the upper photosphere and the chromosphere.

The solar corona is a hot upper atmosphere above 10,000 km of the transition zone. In the transition zone over the chromosphere, the temperature increases from a couple of thousand to around a million kelvin. Therefore, the gas in the corona is hot enough to get away from the Sun's gravity. As a result, the corona begins to flow outward as the solar wind and permeates the entire solar system. It have been proven that the radiation originates in the lower and cooler parts of the solar atmosphere that is the transitional region between corona and chromosphere (Bonnet, 2004; Christiansen et al., 1960).

Reaching down 200,000 km beneath the photosphere is the convection zone, where the Sun's matter is in constant convective movement. Beneath convection zone lies the radiation zone, in which solar energy travels outward as electromagnetic radiation. The term solar interior refers to both the radiation and convection zones. The fundamental interior regions of the Sun are the core, approximately 200,000 km in radius, where intense nuclear reactions produce enormous energy output.

2.2 Solar Activities

Solar activity is a sudden release of stored magnetic energy that accelerates the hot gases near the surface or in the corona of the Sun in all forms such as light, solar wind and energetic particles. The activity varies with time and position on the Sun and indirectly reflects the changes underneath the Sun's surface. The solar activity depends on the rotation of the Sun whether it speeds up or slowing down. It has been observed, faster rotation is diminishes the activity while slower rotation enhances the activity (Landscheidt, 1984). The solar cycle is a periodic 11-year change in the level of solar activity. It shows a solar maximum and solar minimum phase, which indicates the

maximum and minimal solar activity respectively as well as the sunspot number. The most common solar activity phenomena observed are solar flares, prominences and coronal mass ejections (CMEs). Generally, solar activity originates from active regions that is associated with grouping of sunspots. As these solar activities the major part in this study, each of the phenomena are described in the next sub-chapters.

2.2.1 Sunspot

Sunspots are dark areas on the Sun. Basically, it measures about 10,000 km across, approximately the size of the Earth. This region is little cooler than the surrounding photosphere with explosive magnetic field that are confidentially companion with the solar flares and coronal mass ejections. Sunspots show umbra, a center surrounded by brighter penumbra as shown in Figure 2.2. The temperature of the umbra is 37000 K, cooler compared to the penumbra with the temperature of 6000 K. The size of the umbra is ~10,000 km and sometimes can stretch until 60,000 km, while a typical size penumbra is ~5,000 km. The dark appearance on the solar surface is due to the explosive of magnetic fields blocking the creation of the intensity from the solar interior (Hamidi et al., 2015).

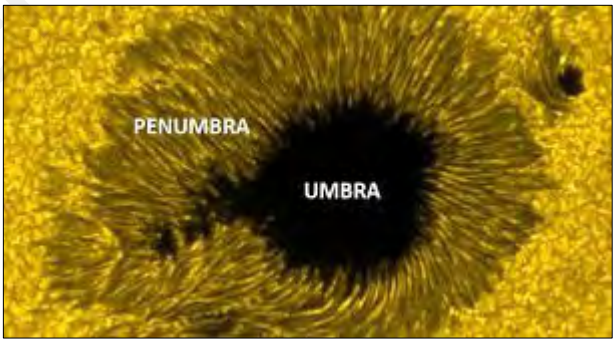

Figure 2.2: An enlarged photo of the largest pair of sunspots.

Sunspot can see alone or in close association with other sunspots, but usually come in pairs and lie at almost the same latitude and have opposites magnetic polarities. As in Earth's magnetosphere, charged particles tend to follow the solar magnetic field lines. Active regions with an official number assigned by NOAA is defined by grouping the

sunspots that are clearly associated with each other. Sunspots change persistently, however singular spots might last for just a couple of hours or for many weeks and even months. The aggregate number of sunspots has quite some time been known to vary with an 11-year period known as the solar cycle. At the solar minimum phase, there can be numerous days in a row with no sunspots visible, while at the solar maximum phase hundreds of spots appear at any one time.

Sunspot groups are the photosphere interface of buoyant magnetic flux ropes, twisted bundles of magnetic flux tubes that are thought to rise through the solar convection zone and into the atmosphere. Sunspots have a characteristic pattern of emergence, evolution and decay. They are also associated with solar eruptions (Higgins, 2012). The polarity of a sunspot simply demonstrates which way its magnetic field is directed relative to the solar surface.

Prominences are loop or sheets of glowing gas ejected from the active regions on the solar surface. It moves through the inner parts of the corona under the influence of the Sun's magnetic field. Magnetic instability found in and near sunspot groups may cause the prominences.

2.2.2 Solar Flare

Solar flares are a phenomenon of sudden brightening observed at the lower solar atmosphere near the active regions. It is a discharge of grand explosion of electromagnetic radiation from the Sun lasting from minutes to hours. The particles delivered are energetic to the point that the Sun's magnetic field is incapable to hold them and move quickly over an area of the Sun in minutes by discharging huge amounts of energy. The unexpected explosion of electromagnetic energy occurs at the speed of light. Solar flares are typically associated with sunspot groups.

Basically, solar flares are seen at optical, radio and X-ray wavelengths. However, the solar flares observed by X-ray wavelength are a good measure of the energy release by solar flares. The solar flare intensities covering an expansive range and are characterized in terms of peak emission in the 0.1-0.8 nm spectral band recorded by the NOAA GOES Soft X-ray instrument. The logarithmic CMX flux scale was used, where C, M and X correspond to fluxes power of 10^{-6}, 10^{-5} and 10^{-4} Wm^{-2} respectively.

Generally, solar flares originate in areas near sunspots. Typically, solar flares last about 20 minutes. In some cases, it takes a couple of seconds to start and lasts up to 4 hours. Numerous solar flares happen in conjunction with a coronal mass ejection (Goss, 2013). However, solar fares can be observed without a CME and CME also can happen without the onset of a flare. The solar eruptive event is when large solar flares and fast CME occur simultaneously (Holman, 2012). There is also some argument about the solar flare and CME by saying that both are the same event. However, from personal communications with Professor Jun Lin from Yunnan Observatory, China on 2014 at the meeting room in the Physics Department, Faculty of Science, University of Malaya clarified this issue. He states that the solar flares and CME are the same process but produce a different product that is expelled from the same level of the solar surface. The contras between the two types of explosions can be seen through solar telescopes, with flares showing as a splendid light and CME appearing as gigantic fans of gas swelling into space.

Energetic particles that consist of electrons and protons were accelerated by the solar flare are detected at the Earth after a delay of minutes to days. The connection between solar radio burst with solar flares was established at the Radiophysics Laboratory (RPL) in Australia in the years of 1946-1952. The very first solar flares written in history was found on 1st September 1859 by the English astronomer, Richard Carrington. Then, it was

confirmed by another English observer, Richard Hodgson. A noticeable geomagnetic storm was detected about a day later beside auroras. Therefore, it is believed that this solar flare may have been standout amongst the most powerful solar flares ever observed (Goss, 2013).

Solar flares can last from minutes to hours and contain tremendous amounts of energy. Traveling at the speed of light, it takes eight minutes for the light of the solar flares to reach Earth. Some of the energy released in the solar flares also accelerates very high energy particles that can reach Earth in tens of minutes.

2.2.3 Coronal Mass Ejection (CME)

A Coronal mass ejection (CME) is a massive scale coronal structure ejected from the Sun's corona and propagate into interplanetary space (Hamidi et al., 2014). Certain CME move toward the direction of the Earth and cause space weather when it intersects the Earth's orbit. Fast CME eruptions are often accompanied with solar flares and filament eruptions. These sudden events include increases in the solar X-ray radiation that cause radio blackouts. Traveling over a million miles per hour, the hot material called plasma takes up to three days to reach Earth.

The commencement of geomagnetic storms and aurora are starts right after the CME impact the Earth's magnetosphere. On the solar surface, CME originate from a highly twisted magnetic field structures or known as flux ropes as shown in Figure 2.3. Often associated with CMEs are filaments or prominences which are relatively cool plasma caught in the flux ropes in the corona. Furthermore, they are always joined by powerful solar flares when these flux ropes expel from active regions.

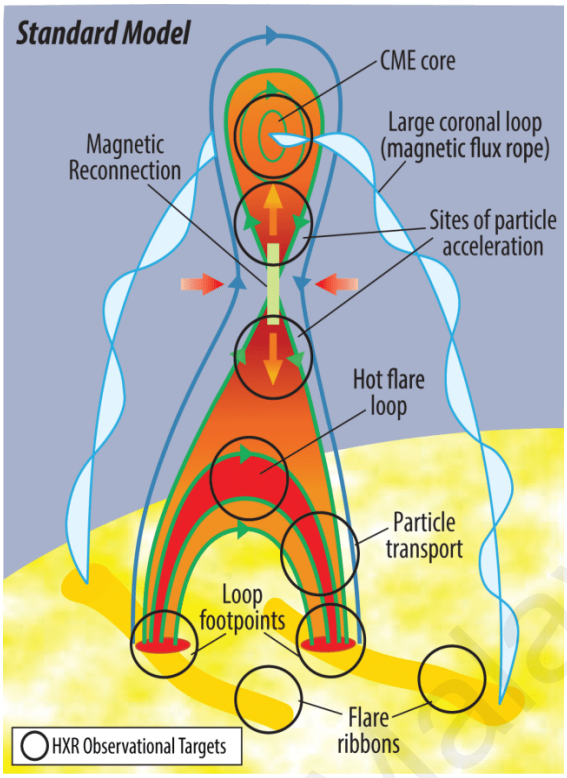

Figure 2.3: A standard model of solar eruptive events observed using HXR (Christe et al., 2017).

Halo CME is a projection effect started near the disk center with a 360 degree of apparent angular width, thus probably moving the component along the Sun-Earth connection line. It appears as a halo because the CME is directed towards the imaging device in the occulting disk imager. A partial halo indicates that the CME was not centered with respect to the imager. It is whether a CME can intersect the Earth depending upon its propagation direction in the heliosphere.

2.2.4 Solar Wind

Solar wind is an outflow of energetic charged particles that persistently streams outward from the Sun and pervades the whole solar system (Chaisson & McMillan, 2014; Gary & Keller, 2004). In fact, solar wind has a different speeds and densities based on the different region on the solar surface and results from the high temperature of the corona.

The solar wind escapes from the low-density regions of the corona called coronal holes. Coronal holes are a region where the magnetic field lines extend from the solar surface far out into the interplanetary space It has been known since the 1960, that a pervasive wind streams out from the Sun with speeds of 300 – 800 km/s. Due to coronal holes, the solar wind speed increases from 500 to 800 km/s and reaches Earth in a couple of days. High latitudes are loaded with rapid solar wind at the north and south poles as they have voluminous and tenacious coronal holes. However, on the equatorial plane, the solar wind speed is slow at around 400 km/s. Consequently, this circumstance of the solar wind shapes the tropical current sheet (Higgins, 2012).

Besides, the current sheet can be closely flat during quiet periods. Solar wind and current sheet undergo a change when the solar activity increases. As solar activity increases, the solar surface is peppered with coronal holes, active regions and other complex structures. Since the Sun revolve every 27 days, the solar wind turns into a complicated spiral fluctuation of speeds and density that resembles the skirt of a spinning ballet dancer. Corotating interaction region happens when the high velocity solar wind overtakes slow speed wind, and this region consists of solar wind with high densities and forceful magnetic fields.

Over the current sheet, the advanced velocity solar wind commonly has a predominant magnetic polarity in one way and underneath the current sheet, the polarity is in the opposite direction. As the Earth travels through this advancing ballerina skirt, it is in some cases inside the heliospheric current sheet, occasionally above it and at some point, underneath it. There is strong indication that Earth has crossed the current sheet when the magnetic field of the solar wind switches polarity. The area of the Earth within the current sheet is consequential because space weather affects are profoundly reliant on the solar

wind speed, the solar wind density, and the direction of the magnetic field embedded in the solar wind.

2.2.5 Geomagnetic Storm

Geomagnetic storm is a major disturbance on Earth's magnetic field that occurs when a very efficient exchange of energy from the solar wind into the space environment surrounding the Earth. These storms result from variances in the solar wind that produces major changes in the currents, plasmas and fields in Earth's magnetosphere. The solar wind conditions that are effective for creating geomagnetic storms are sustained (for many hours) periods of high-speed solar wind.

Geomagnetic storms are also defined as a change in the disturbance storm time (Dst) index. It widely used to describe the measure of a geomagnetic storm. In any case, there are currents produced in the magnetosphere that take after the magnetic field and connect to intense currents in the auroral ionosphere. These auroral current create large magnetic disturbances on the ground used to produce a planetary geomagnetic disturbance index called k_p. This index is used globally to portray space weather that can disrupt systems on Earth. The mean planetary k_p index for geomagnetic storm is nT with interval for 3-hours. The k_p-index ranges from 0 to 9, where the value of 0 implies very little geomagnetic activity and a value of 9 implies an extreme geomagnetic storm. For geomagnetic storm, it has 5 indexes of k_p beginning from level G1 (minor storm), G2 (moderate storm), G3 (strong storm), G4 (severe storm) and G5 (extreme storm).

2.3 Impact of Solar Activity to Space and Ground Technology

The Earth's surrounding known as Space Weather is the condition of the solar wind speed and density, magnetic field strength and orientation, and energetic particle levels (White, 2007). The high energies and magnetic field strengths from the Sun streams at

thousands of km/s impact the Earth's magnetosphere and might be harmful to the Earth technology (Balogh et al., 2007).

The energetic particles release energy into the ionosphere in the form of heat that may drive the system to encounter surface charging, thus dragging the satellites in low-earth orbit and orientation problems may occur. The local heating also creates strong horizontal variations in the ionospheric density that can modify the path of radio signals and create errors in the positioning information provided by the Global Positioning System (GPS). Consequently, it disturbs the navigation systems for example, the Global Navigation Satellite System (GNSS) as well as creating a harmful geomagnetic induced currents (GICs) in the electrical power grids and pipelines.

Thus, the relationship between solar radio burst with solar activity plays a beneficial role in space weather study. The information gathered from the relation of type III and type IV solar radio bursts with solar activity might be worthwhile in order to predict the impact of solar events on our technology.

2.4 Solar Radio Burst

Solar radio burst was among the primary wonders recognized as new focuses for radio astronomy. A solar radio burst is a structure in frequency that changes with time. They are characterized depending on bandwidth, frequency drift rate and life span of the emission. There are five (5) main types of solar radio burst at frequencies below a couple of hundred MHz which is type I, type II, type III, type IV and type V (White, 2007). The solar radio burst data were displayed in the spectrogram which have frequency, time and intensity. It is accredited that these bursts are prompted by beams of fast electrons at levels of the local plasma frequency or its second harmonic. Figure 2.4 demonstrates the types of solar radio burst emission released from the solar surface.

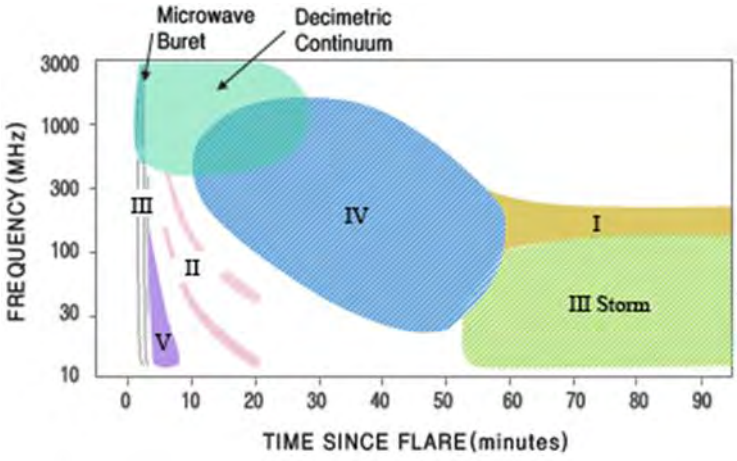

Figure 2.4: Classification of solar radio bursts.

2.4.1 Solar burst type I

Type I consists of a continuum component that are non-flare phenomenon. It is otherwise called a "noise storm" and covers the frequency range from 100-400 MHz and often occurs for hours. Type I solar radio burst normally has a bandwidth of several MHz and its long span is from 0.1 seconds to 1 second (Monstein, 2015). It is outstanding that type I solar radio burst have extended lifetimes due to energetic electrons trapped in closed coronal magnetic field lines.

2.4.2 Solar burst type II

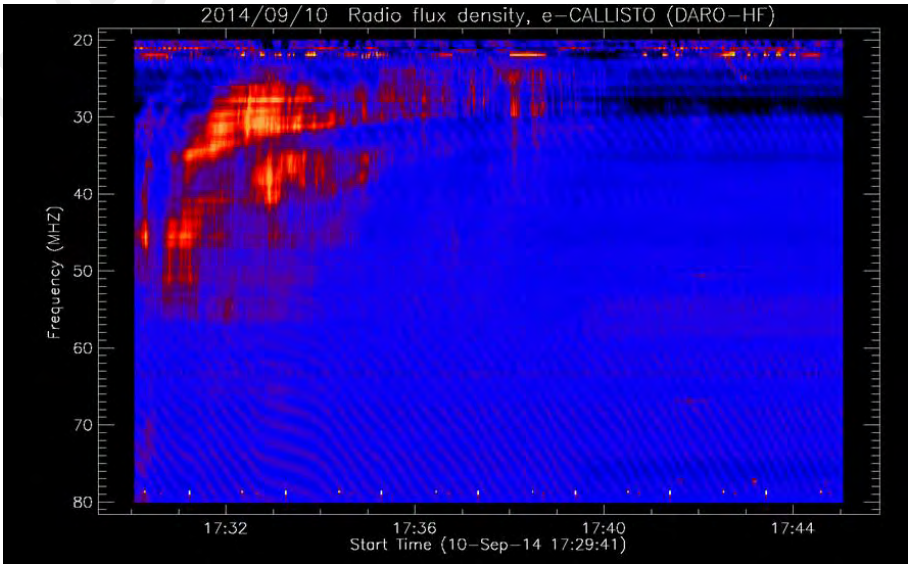

Figure 2.5: An intense herring bones feature of solar radio burst type II.

Solar radio burst type II can be identified based on the slow frequency drift burst. It sometimes it appears like herring bones feature (Figure 2.5) with a duration of about 3-30 minutes occurring at a frequency range from 20 – 150 MHz. It is believed that the electron accelerated by magnetohydrodynamic shocks driven by solar eruptions is the main cause to the formation of type II solar radio burst (Kong et al., 2012). Moreover, type II solar radio burst simply can be recognized by the narrow stripes in the metric to kilometric wavelength range. It drifts gradually from high frequency to low frequency because of an outward propagation of the electron source along with the shock (Nelson & Melrose, 1985; J. Wild, 1950). Type II solar radio burst consists of fundamental (F) and the second harmonic (H) emissions that are separated by a frequency gap and were produced by plasma radiation mechanism at frequencies determined by the local plasma density (Ginzburg & Zhelezniakov, 1958). The frequency drift rate of this burst is beneficial in order to get the shock propagation speed by changing over the emission frequencies into coronal heights by assuming a coronal density model (Cho et al., 2007; Reiner et al., 2003; Vršnak et al., 2001; Vršnak et al., 2002; Vršnak et al., 2004).

2.4.3 Solar burst type III

Solar radio burst type III is generated from the fast electron particles ejected from the Sun. One of the trademark type III solar burst is the rapid drift of frequency from high to low that was attributed to the decrease of electron plasma frequency (Lin et al., 1981). Furthermore, type III burst can occur singularly with a duration of 1 – 3 seconds, in groups for 1- 5 minutes or storm which is usually long lasting, intense bursts seen in the low-frequency observations. The example of single and storm type III solar radio burst can be seen in Figure 2.6. It is generally accepted that it caused by streams of electrons travelling along open field lines from the flaring regions near the Sun into the interplanetary medium (Cane et al., 2002; Hamidi et al., 2014).

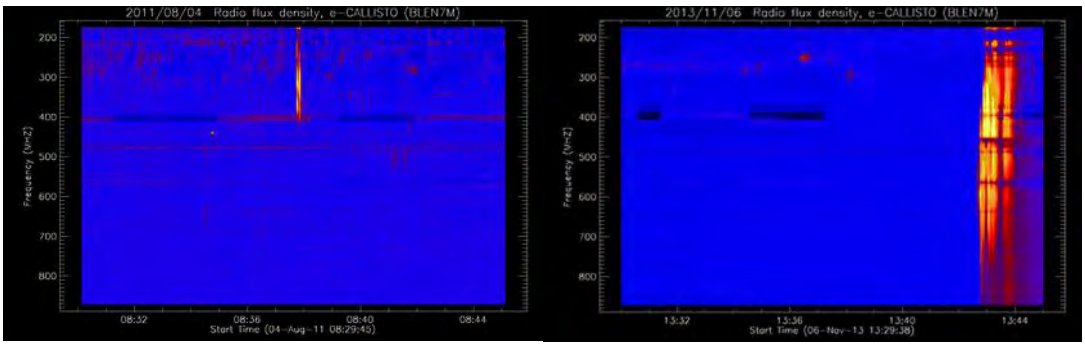

Figure 2.6: An example of single (left) and storm (right) solar radio type III burst.

Type III solar radio bursts has the fastest drift rates of bursts at metric wavelengths and was made by an electron beam through plasma emission. The radio emission tracks the electron beam as it goes past the diminishing plasma density of the solar corona and solar wind. Type III solar radio burst basically starts at the frequency above 100 MHz. Consequently, drift downward in frequency happens as the driving electrons move out into the undeniably weaken plasma of the solar wind. However, it hard to find the fundamental hormonic structure of type III solar radio bursts. It is very much acknowledged that type III solar radio bursts are highly couple with electron beams. These beams drive an electrostatic Langmuir waves that are also known as bump-on-tail distributions (Cairns et al., 2000). Hence, the radio emission produced tends to be extremely erratic with electric fields that often vary by more than two orders of magnitude from one sample to the next.

2.4.4 Solar burst type IV

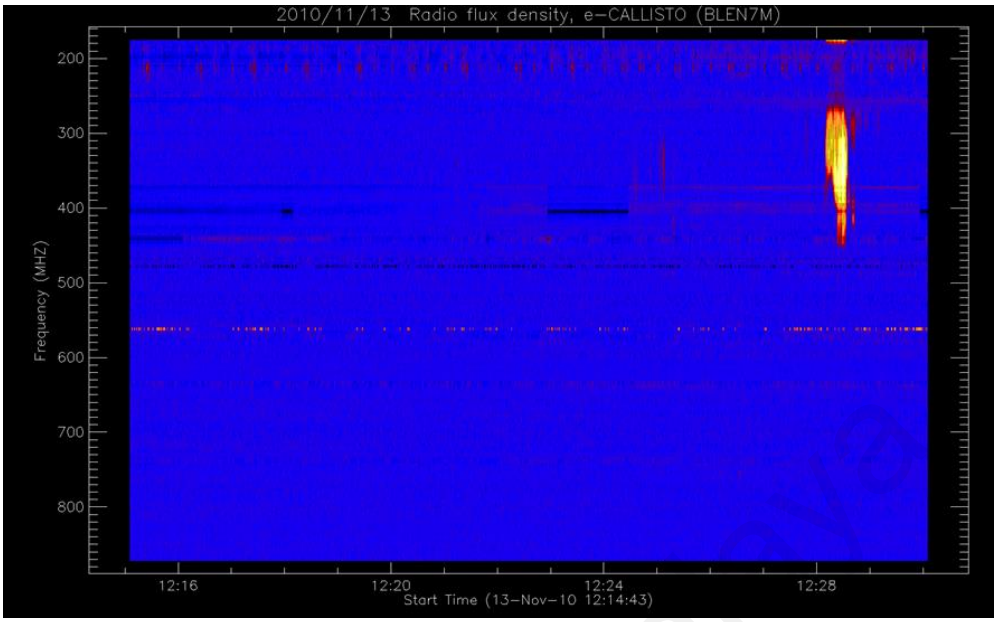

Figure 2.7: An example of solar radio burst type IV.

A smooth broadband quasi-continuum features associated with the decay phase of solar flares is one of the characteristic of type IV solar radio bursts (Fokker, 1963; White, 2007). Type IV solar radio bursts emission has a duration from a couple of minutes to a couple of hours. As can be observed, it covers a wide range of frequencies and generally varies smoothly in both time and frequency (Bell, 1963b). It generally believed that type IV solar radio bursts generates from the synchrotron radiation of relativistic electrons spiraling in magnetic fields (Bell, 1963b; Pick & Vilmer, 2008) and a results from trapped in accumulating accelerated electrons (Zlotnik et al., 2005).

Generally, type IV solar radio bursts were classified into 3 groups; which are stationary, moving and flare continua. Moving type IV bursts in metric and decametric frequencies are emitted by the gyro-synchrotron mechanism from mildly relativistic electrons (Nelson, 1977), which are accelerated in flares, by their interaction with sunspot magnetic fields being stretched outwards (Sakurai, 1973). Continuum type IV solar radio burst are mostly associated with solar flares. At the centimeter-wavelength bursts, type

IV solar radio burst are closely coupled with solar flares, especially the extreme ones (Kundu, 1965).

Furthermore, type IV solar radio burst are always related to the development of sunspot groups (Antalová, 1967). It has been well established that type IV bursts have a high probability of being followed by geomagnetic disturbance (Cane et al., 2002).

2.4.5 Solar burst type V

The Type V solar radio burst was first defined (Wild et al., 1959) as a wide bandwidth, continuum burst with a duration of between 1 and 3 min. This burst is very comparable and forms after type III solar radio burst with difference of few seconds. The radiation is generally restricted to frequencies below 150 MHz (Wild et al., 1959) and has a bandwidth which is a substantial fraction of the central frequency and generally decreases with time. This type is additionally identified with the development of coronal mass ejections however, has received very little attention by space researchers.

CHAPTER 3: LITERATURE REVIEW

3.1 Magnetic Reconnection

It is broadly acknowledged that the magnetic reconnection is the one mechanism, in releasing the energy stored in sheared magnetic fields on its surface. Magnetic reconnection is a process where the oppositely directed field lines come closer and join, thus resulting in the release of the magnetic energy in the form of thermal energy and particle acceleration (Kumar & Manoharan, 2013).

The Sun has a very weak magnetic field (average dipole field). Nonetheless, the Sun has extremely powerful and enormously complicated magnetic fields. Figure 3.1 illustrates the way the Sun's corona was heated by its "magnetic carpet". When magnetic field lines join at the north and south poles in the "magnetic carpet" it produces the loops that extend into the corona.

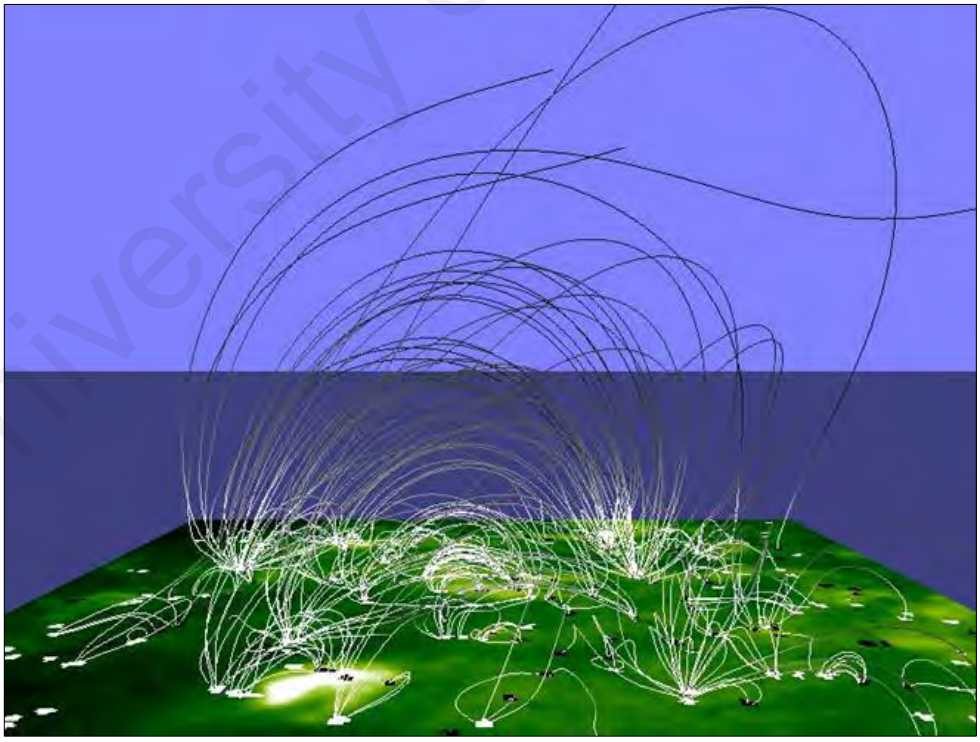

Figure 3.1: Magnetic field on the Sun. Credited to NASA.

In addition to observing the reconfiguration of magnetic structures in the atmosphere, Figure 3.2 demonstrates the process of solar flare formation by the sudden release of energy when powerful magnetic fields reconfigure and reconnect. The yellow arrows show the direction of the plasma during the eruption.

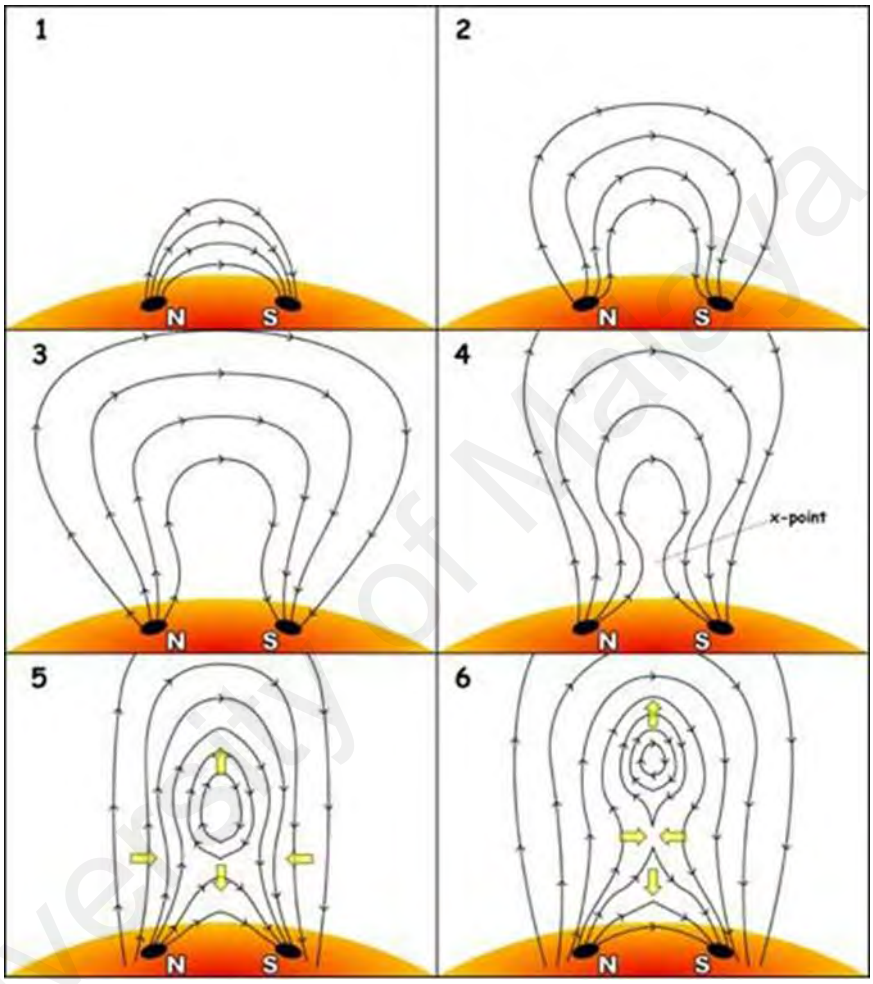

Figure 3.2: Process of magnetic reconnection. Credited to University of California.

Magnetic reconnection occurs when a magnetic field rearranges itself to move to a lower-energy state. Magnetic force is a "push" or "pull" on the on the object with moving electric charges. Magnetic field occur when the electron inside the magnets are spinning in the same direction. Polarity of the magnet, namely north and south poles produces a self-created field. Magnets repel when the same poles are close to each other and reconnect on the opposite polarity, thus suddenly converting the magnetic energy into

thermal and kinetic energy. As shown by a pair of magnets, the movement of electric charge is the driving force of magnetism.

Reconnection occurs wherever charged gases (plasma) are present. Plasma happens at high temperatures where electrons are no longer bound to the nucleus, thus ions and electrons can move freely. The free movement of charges results in a highly conductive plasma, hence causing the magnetic field lines to "freeze" into the plasma. In reconnection, smooth movements in plasma unite two "frozen" and oppositely coordinated magnetic field lines. Therefore, these fields reconnect into a lower energy state. Because of the smooth movements, the "frozen" field lines become distorted and the energy was stored in reconnection (Bak, 1993). Energy will be released when the amount of distortion lessens in the reconnection process.

This process is believed to be behind the sudden releases of energy from the solar surface in the form of solar flares and CME. Both eruptions are created when the motion of the Sun's interior contorts its own magnetic fields like a sudden release of a twisted rubber band. The magnetic fields will explosively realign, driving huge amounts of energy into interplanetary space. In some cases, solar magnetic field is entrenched in the plasma and streams outmost with the solar wind.

3.2 Solar Radio Emission

The solar radio emission in meter and decimeter wavelengths brightens up by several orders of magnitude during the solar flares. These radio sources outshine the thermal radiation to the rest of the Sun called a burst. The most common characteristics of these emissions are that they are not produced by single electrons as in free-free emission (bremsstrahlung radiation) or synchrotron radiation, instead by waves and instabilities in the plasma. The wave presents an organization in the plasma that enables particles to discharge in phase coherently (Benz & Saint-Hilaire, 2003).

Coherent emissions are for the most part extremely effective in converting kinetic particle energy into radiation. Thus, it results in a bright coherent emission and indicates the presence of waves in the plasma. The waves that can raise escaping radio emissions should have a high frequency. The frequency must be above the local plasma frequency and are basically energized by some instability. Accordingly, coherent emissions show the presence of a cause for instability, for example, a beam of electrons, magnetically trapped electrons having a loss-cone velocity distribution, a shock, or an unstable current (Benz & Saint-Hilaire, 2003).

For this reason, the Bremsstrahlung radiation, Langmuir wave and Moreton wave are explained briefly in the following sub-section by describing how the solar events convert to electromagnetic emission.

3.2.1 Bremsstrahlung Radiation

An intense radiation during solar flare occurs in all wavelengths of electromagnetic spectrum. Half of the energy discharged during flares is used to accelerate electrons and protons up to the speed of light, hurling them out into the interplanetary space. The energy of the photons is emitted typically in the X-ray range, classified as hard X-ray (10-100KeV) emissions and soft X-ray (~0.1-10 keV) emissions. Generally, whenever a charged particle is accelerated, electromagnetic radiation is produced. If the charged particle is accelerated at very high velocities, the emitted photon produced has a higher energy.

There are two general types of electromagnetic radiation which is thermal and nonthermal (Moreton, 1964). Thermal radiation relies on the temperature of the emitting source while nonthermal does not rely on the source temperature. The thermal radiation processes are black body radiation and thermal bremsstrahlung (Kumar et al., 2015). The non-thermal emissions are non-thermal bremsstrahlung, inverse Compton scattering, and

synchrotron radiation X-ray and radio emission mechanism can be classified as coherent and incoherent emissions (Burkhardt et al., 1998).

Both thermal and non-thermal radiations occur in solar flares (Kumar et al., 2015). The hard X-rays are generally accepted to be non-thermal bremsstrahlung emission produced by high-energy electrons precipitating into the chromospheres. Fast electrons that are thrown down into the Sun emit hard X-rays when entering the lower solar atmosphere (Lang, 2009). An illustration of X-ray photon production in solar flare is shown in Figure 3.3.

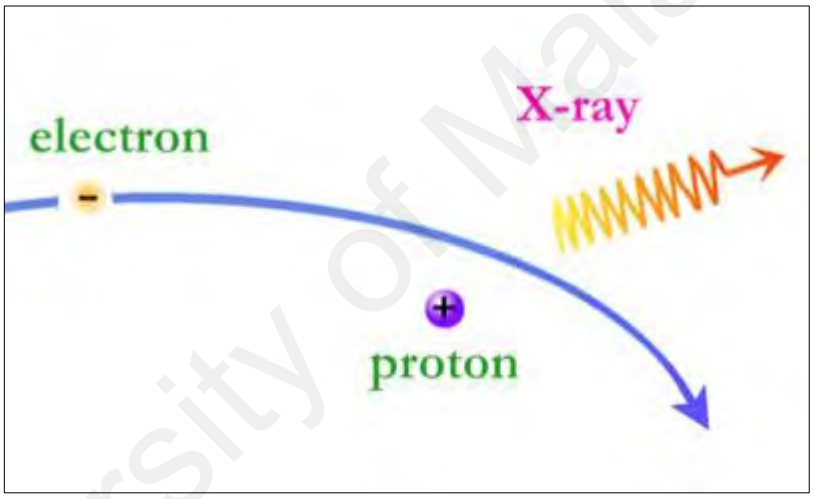

Figure 3.3: Production of X-ray in solar flare.

In contrast, radio emissions are due to relatively gentle, distant collisions of electrons with ions. Bursts at the centimeter wavelengths of radio emission and X-rays occur at the same time during solar flares. The high energy of the X-ray bursts are due to nonthermal bremsstrahlung radiation (Kundu, 1965).

Nonthermal electrons that traveling away from the Sun along open field lines produce type III radio solar bursts and storms over an extensive range of wavelengths (Bougeret et al., 1984). These are generally lower energy electrons ($\leq$ 10 keV). Electrons accelerated

at the flare site and trapped in moving and stationary magnetic structures produce type IV bursts (Gopalswamy, 2016).

3.2.2 Langmuir Wave

Plasma oscillation or Langmuir waves are a natural mode of a plasma excited by a variety of mechanisms (Melnik et al., 2011). The excitation of Langmuir waves near the local electron plasma frequency are due to the electron beams travelling inside the solar corona (Hamidi, 2014). At the point when these Langmuir waves are regenerate into electromagnetic waves, the radiation of the burst can be seen at the radio region with a unique structure. Usually, the proportion of closed to open magnetic field structures rise with lower altitude.

Langmuir waves were first proposed in that these bursts are probably excited by the plasma mechanism (Ginzburg & Zhelezniakov, 1958). It consists of (1) the flare accelerated electron beam, while propagating radially outward in the solar atmosphere, excites Langmuir waves in a very narrow band around the local electron plasma frequency, $f_{pe} = 9n_e^{1/2}$, by a mechanism known as bump-on-tail instability (Bohm & Gross, 1949), where n_e is the electron density in m^{-3}, and (2) subsequent conversion of these Langmuir waves into electromagnetic waves at the fundamental and second harmonic of the electron plasma frequency, f_{pe}. (Li et al., 2008; Thejappa et al., 2012; Thejappa et al., 2012).

It been well understood, the spectrum that defines the characteristics of type III solar radio burst is an emission of the frequency that decreases with increasing time. This happens due to the decreasing electron plasma frequency encountered by the solar flare electrons when it streams outward from the Sun (Gurnett et al., 1993; White, 2007).

3.2.3 Moreton Wave

Moreton wave is a shock wave in the Sun's chromosphere produced by a large solar flare as shown in Figure 3.4. It can expand outwards with the speed of around 1,000 km/s, and typically presents itself as a gradually moving diffuse arc of brightening H-alpha or coronal line. This Moreton wave can travel for several hundred thousand kilometers and constantly couple with the solar radio bursts at meter wavelength. It was named after the American solar astronomer Gail Moreton (Narukage et al., 2004).

Moreton waves is a large-scale disturbance which happens at Sun's atmosphere and is related to solar eruption phenomena such as coronal mass ejection and solar flare. In a study at Hida observatory, they found out that more than 10 Moreton waves have been observed associated with about 10% of X or M -class flares.

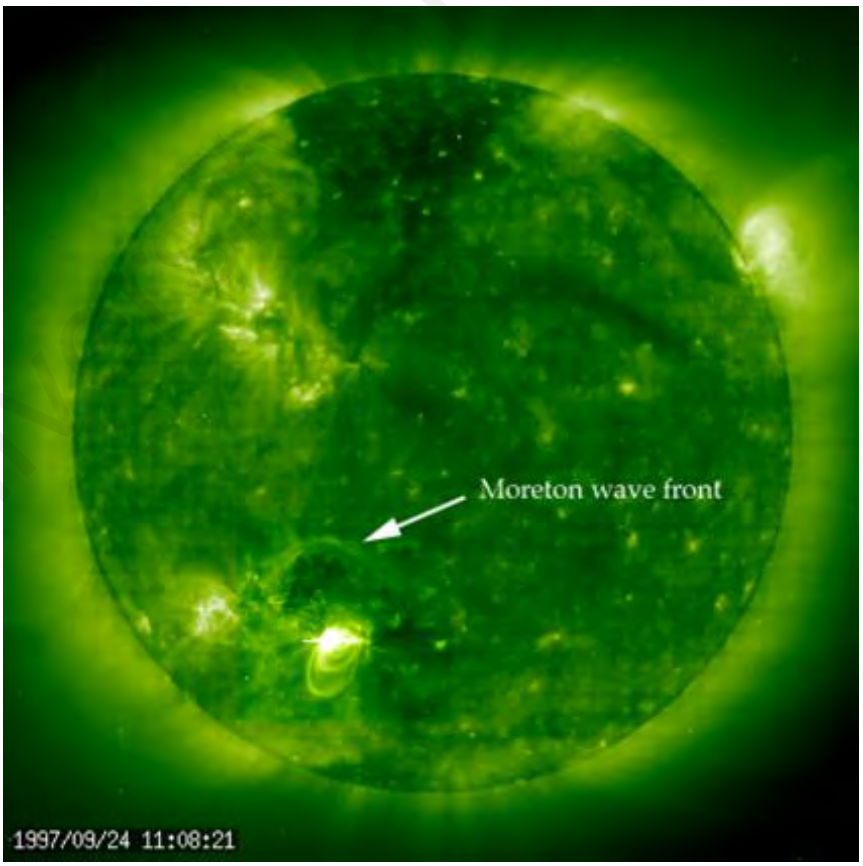

Figure 3.4: Moreton waves from AR 8088, 1997 September 23.

3.3 Radio Frequency Interference (RFI)

Radio frequency interference is the most serious issue that needs to be addressed for solar monitoring activities with regards to ground-based telescopes including CALLISTO. According to Ellingson (2005) man-made radio signals can be detected throughout the radio spectrum. It varies by time and frequency and adequately to be track down in the far-outside lobes from the main beam response of the antenna.

Radio frequency interference can be defined as a conduction or radiation of radio frequency energy that causes electronic or electrical devices to produce noise which interferes with the functionality of the adjacent device by disrupting the normal functioning of electronic and electrical devices. Besides that, RFI occur naturally as well as intentionally. Solar storm that effect the satellite communication is considered as a natural radio frequency interference, while man-made interference is intentional radio frequency interference.

The radio frequency interference can be divided into two classes which is external and internal radio frequency interference. External radio frequency interference comes from the surrounding environment from all kinds of radio application such as radio broadcast, transient interference like radars and aviation radio broadcast. All of the interference can be avoided by choosing the Radio Quiet Zone (RQZ) location for observation (Umar et al., 2014). While for internal radio frequency interference comes from radiating devices such as computers, scientific instruments, electrical motors, microwave ovens and many more. These harmful radiators are located very close to the radio telescope and the receiver (Porko, 2011).

It became a major problem when radio frequency interference disrupts the important information about the data by unwanted radio frequency signals as shown in Figure 3.5. However, a few procedures have been found to exclude the RFI, which is knowing as the

post-correlative projection matrix method (Kocz et al., 2010), blanking and coherent subtraction.

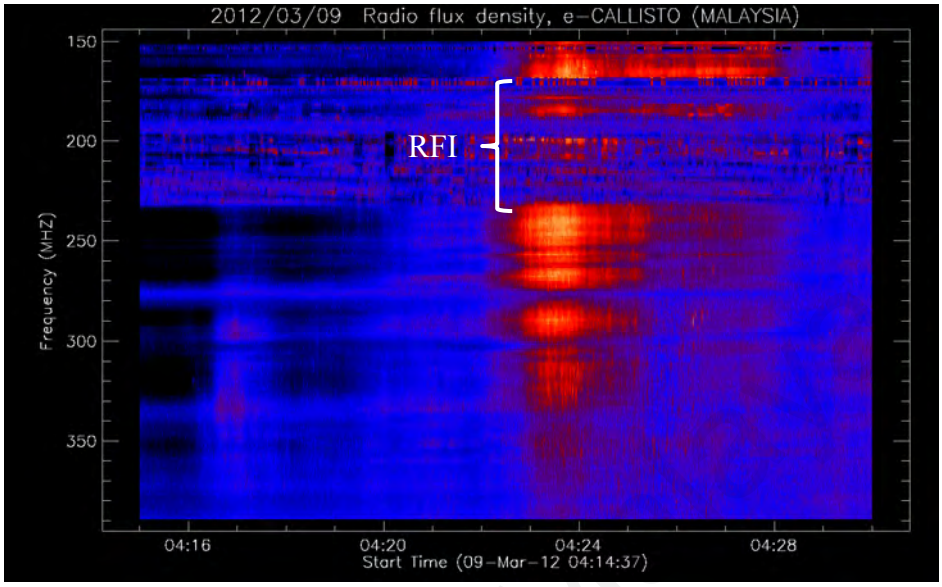

Figure 3.5: Example of RFI disturbing the type III solar radio burst on 9th March 2012.

For CALLISTO spectrometer, Christain Monstein the project manager of the CALLISTO has compiled and analyzed spectral overviews from several stations. the spectral overview is a useful for reference of possible interference sources for the other CALLISTO stations setup, RFI mitigation and detection. Figure 3.6 and Figure 3.7 shown RFI of all the sites of the CALLISTO network and two-dimensional skewness level in RFI over the whole spectrum during 15 minutes of observations (without solar bursts) respectively.

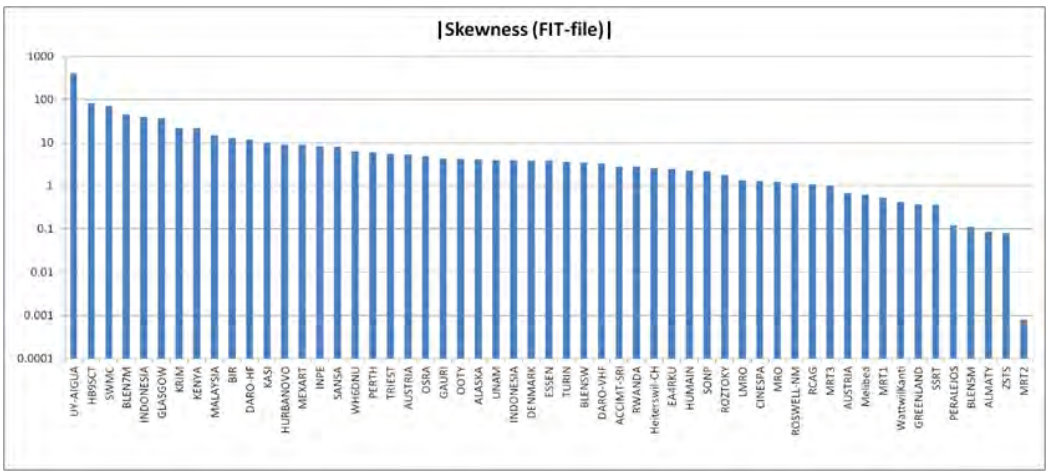

Figure 3.6: RFI of all the sites of the CALLISTO network.

The disturbance level is taken from single a 15-minute FIT-file per location of the e-Callisto network in April 2016. As seen from the Figure 3.6, Uruguay shows the highest levels of RFI interruptions while the MRT-2 stations in Switzerland indicate low levels of interference out of 55 stations.

Skewness is a measure for the deviation from the Gaussian noise distribution. The overall quality of the data is better generally if the skewness interference level is low. But it does not inform anything concerning the sensitivity of an individual instrument with regards to a solar burst. Sensitivity concerning solar bursts strongly relies upon whether the instrument is connected to a large or a small antenna (Ramli et al., 2015) and whether it can be positioned facing the Sun.

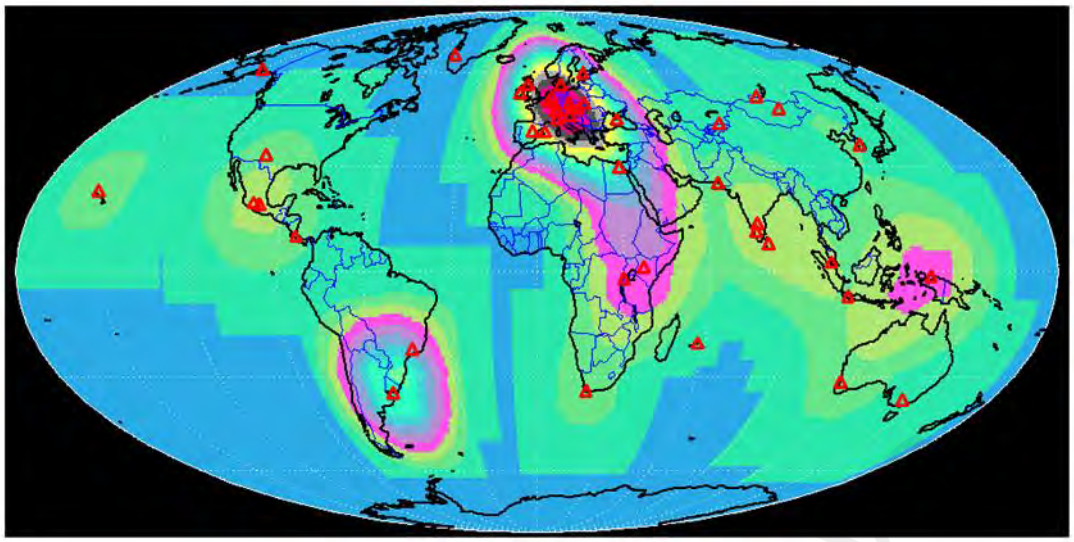

Figure 3.7: Purple areas in the left map denote to a two-dimensional skewness level in RFI over the whole spectrum during 15 minutes of observations (without solar bursts).

There is a study from Abidin et al. (2015) that explores the common development of RFI on the spotting of solar radio burst by using CALLISTO. The Overview Spectrum (OVS) from the 23 stations (until 2013) was collected to see the RFI effect on the each CALLISTO stations. Then, it was grouped from 45-200 MHz, 200-400 MHz, 400-600 MHz and 600-870 MHz for comparison of their interference level. The average RFI of all stations from 45-870 MHz was compiled as shown in Figure 3.8. By using the blanking technique in the RAPP software in CALLISTO, it obviously shows that CALLISTO stations should be competent to observe solar radio activity in the frequency windows of 45-80MHz, 240-380MHz and 780-850MHz.

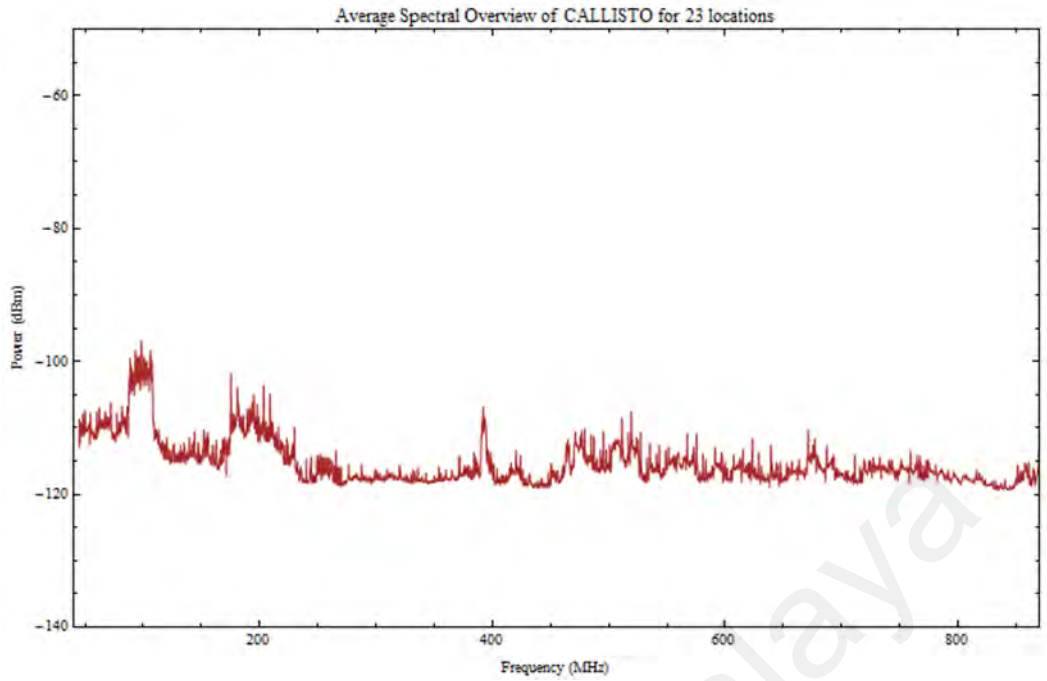

Figure 3.8: The average RFI power of all 23 stations using the OVS between 45 MHz to 870 MHz.

Other than that, they had discovered that the RFI severely affects CALLISTO within radio astronomical windows below 870 MHz (in the ranges of 80-110 MHz and 460-500 MHz). All the stations are relatively free from RFI at 270-290 MHz.

There is spectrum allocation provided by each country to recognize the sources of RFI. Spectrum allocation is the allocation and regulation of the electromagnetic spectrum in the radio bands. Also known as spectrum management or frequency allocation, it was set by governments in most countries (Mazar, 2009). International Telecommunication Union (ITU) is a specialized agency of the United Nations (UN) is the one responsible in providing global radio spectrum allocation for reference.

CHAPTER 4: RESEARCH METHODOLOGY

4.1 The Methodology Flow Chart

Figure 4.1 presents the methodology flow chart of this research. The process starts with the literature review, giving a deeper understanding of the essentials of the Sun and the instrument being used in this research.

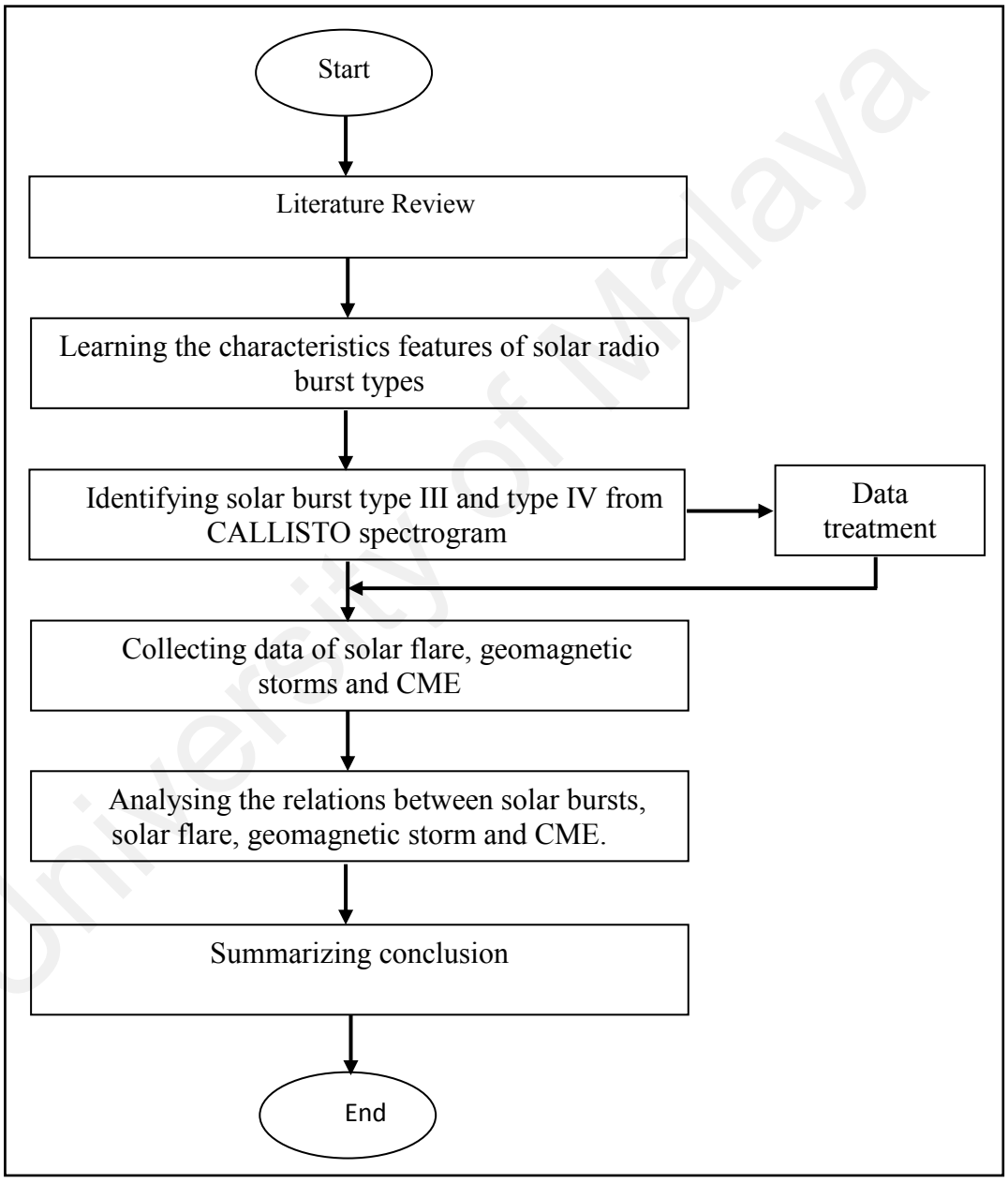

Figure 4.1: The research methodology flowchart.

Other than that, there is a need to learn the characteristics of each solar radio burst. This takes extensive time to differentiate the features of any solar radio burst as many aspects must be taken into consideration. After that data is collected from the e-Callisto website. This step takes a lot of time because of the need to go through the data one by one for each day, with more than 1000 data per day. Then, the data treatment was done to eliminate the noise to get an accurate reading of frequency and time by using Python software. All the solar radio burst type III and type IV data was compared with the solar flare, CME and geomagnetic storm. Finally, the data was analyzed to find their relationship.

4.2 Instrumentation

The solar radio burst types III and IV were observed by the CALLISTO Spectrometer. CALLISTO is an acronym of Compound Astronomical Low cost Low frequency Instrument for Spectroscopy and Transportable Observatory. The CALLISTO spectrometer was designed by an electronics engineer, Christian Monstein from the Institute for Astronomy of the Swiss Federal Institute of Technology Zurich (ETH-Zurich). The radiometric bandwidth is about 300 kHz and the integration time for this spectrometer is 1 msec with 0.25 sec time resolution of 200 channels per spectrum (800 pixels per second). The instruments were placed at a low-noise level location to reduce the system noise and the preamplifier was connected to the spectrometer, to amplify a gain. In term of the sensitivity, it is dependent on the instrument whether it connected to a small or large antenna.

This spectrometer will detect the intensity of electromagnetic radiation at radio frequencies between 45 until 870 MHz (Rathore et al., 2014). At the moment, there are more than 144 instruments in more than 80 locations all over the world including Malaysia. It observes automatically, and the data are collected every day via the internet

and stored in a central database at the Institute for Astronomy of the Swiss Federal Institute of Technology Zurich (ETH-Zurich) (Hamidi et al., 2012). Overall, this major project combines the worldwide data of solar bursts and potentially monitors the Sun with 24 hours coverage. Table 4.1 shows 44 out of 55 current stations and their coverage with the ID file of each site.

Table 4.1: 44 CALLISTO stations coordinates (longitudes and latitudes) and the frequency range covered by their antenna with coverage time. The superscript asterisk indicates approximated value.

No	Site	Latitude	Longitude	Frequency (MHz)	Observation time
1	Daejon, South Korea (KASI)	36.350 N*	127.384 E*	45-870	11h 5m
2	Anchorage, Alaska (ALASKA)	61.218 N*	149.900 W*	45-870	5h45m
3	Mexico (UNAM)	19.332 N	99.188 W	170-450	11h5m
4	Metsahovi, Finland (MRO)	60.218 N*	24.394 E*	170-870	6h45m
5	Essen, Germany (ESSEN)	51.394 N	6.979 E	150-850	7h30m
6	San Jose, Costa Rica (CINESPA)	9.933 N*	84.083 W*	45-870	11h35m
7	Nairobi / Kenya (KENYA)	1.283 S	36.817 E	40-175	12h00m
8	Cachoeira Paulista, Brasil (INPE)	22.665 S*	45.012 W*	45-870	11h00m
9	Bleien, Switzerland (BLEN7M)	47.344 N	8.114 E	170-870	7h45m
10	Czech Republic (OSRA)	49.543 N*	14.465 E*	150-870	8h45m
11	Hurbanovo, Slovakia (HURBANOVO)	47.5 N	18.0 E	45-870	8h45m
12	Ooty, India (OOTY)	11.412 N	76.695 E	45-450	11h30m
13	LMRO, Australia (LMRO_Australia)	36.805 S	144.675 E	45-870	11h30m

Table 4.1, continued.

No	Site	Latitude	Longitude	Frequency (MHz)	Observation time
14	Helwan / Egypt (SWMC)	29.863 N	31.325 E	110- 340	10h30m
15	Humain, Belgium (HUMAIN)	50.205 N*	5.257 E*	45-870	8h30m
16	Bandung, Indonesia (BOSSCHA-ITB)	6.493 S	107.371 E	45-870	12h00m
17	Glasgow, UK (GLASGOW)	55.872 N	4.289 W	45-870	6h45m
18	Kuala Lumpur, Malaysia (MALAYSIA)	2.809 N	101.504 E	150-400	12h00m
19	Roztoky, Slovakia (ROZTOKY)	49.391 N*	21.493 E*	0-900	8h45m
20	Badary, Russia (SSRT)	52.312 N*	104.296 E*	45-450	8h45m
21	Trieste, Italy (TRIEST)	45.654 N	13.778 E	30-450	8h45m
22	Perth, Australia (PERTH)	31.953 S*	115.857 E*	45-870	12h45m
23	Gauribidanur, India (GAURI)	13.672 N	77.782 E	45-410	11h00m
24	Almaty, Kazakhstan (ALMATY)	43.250 N*	76.916 W*	45-870	8h50m
25	SANSA Hermanus, South Africa (HERCLSI)	34.42° S	19.22 E	45-870	10h45m
26	Crimea / Ukraine (KRIM)	44.393 N*	33.972 E*	45-870	9h30m
27	Kigali/Rwanda (RWANDA)	1.974 S	30.114 E	45-870	12h00m
28	Karachi, Pakistan (SONP)	24.918 N	66.923 E	45-870	10h45m
29	Ulaan Baatar, Mongolia (RCAG)	47.921 N*	106.906 E*	175-450	8h45m
30	San Isidro, Lima/Peru (CONIDA_SI)	12.065 S	77.033 W	45-870	12h00m

Table 4.1, continued.

No	Site	Latitude	Longitude	Frequency (MHz)	Observation time
31	Birr, Ireland (BIR, BIRO)	53.097 N	7.914 W	45-870	7h30m
32	Mauritius (MRT, MRT1, MRT2, MRT3)	20.167 S*	57.749 E*	45-870	12h50m
33	ACCIMT, Sri Lanka (ACCIMT-SRI)	6·474 N	79·535 E	45-870	11h45m
34	Roswell New Mexico, USA (ROSWELL_NM)	33.394 N*	104.523 W*	210-450	10h30m
35	Peralejos, Spain (MELIBEA, PERALEJOS)	40.365 N	3.762 W	50-900	9h30m
36	Servicio de Clima Espacial (CALLISTO_MEX)	19.817N	101.583 W	45-870	11h30m
37	Pune, India (PUNE)	18.520 N	73.856 E	45-870	11h15m
38	Wattwil, Switzerlannd (HEITERSWIL)	47.305 N	9.129 E	45-870	8h45m
39	Kangarlussuaq, Greenland (GREENLAND)	66.987 N	309.055 E	10-110	2h
40	Ahmedabad, India (INDIA-KSV)	23.033 N	72.585 E	100-900	10h15m
41	Mekelle, Ethiopia (ETHIOPIA)	13.475 N	39.485 E	50-900	10h30m
42	ANTARES, Michelbach Austria (AUSTRIA)	48.087 N	15.756 E	20-80	8h30m
43	Lustbuhl, Austria (AUSTRIA-UNIGRAZ)	48.210 N	16.363 E	45-82	8h30m
44	Montevideo, Uruguay (URUGUAY)	34.733 S	56.190 W	80-870	10h45m

4.3 Data Collection

The observational data were obtained from the data archive of bursts recorded from e-Callisto using the CALLISTO Spectrometer. It contains the data of all types of solar radio bursts from the year 2006-2011. This study is only focused on solar radio burst type III and type IV. For selected events, only from the best events of solar radio burst type IV that is associated with solar radio burst type III were chosen. This data was collected from the e-Callisto website by going through all the data day by day.

For analysis with solar activities, the solar flare data, solar wind, sunspot and CME were also collected. Solar flare and sunspot data were collected from the National Oceanic and Atmospheric Administration (NOAA) website. Solar flare data was also collected by Geostationary Operational Experimental Satellites (GOES) in the form of X-rays, protons and electrons while the images of sunspot was provided by the XRT satellite. Both data are available online from the solarmonitor.org. The solar wind data consists of velocity and proton density were presented on spaceweather.com and are updated every 10 minutes. It was derived from real-time information transmitted to Earth from the ACE spacecraft and reported by the NOAA Space Environment Center. The location of ACE at the point between the Earth and the Sun enables the spacecraft to give about an hour advance warning of impending geomagnetic activity.

The compilations of CMEs as observed by the Large Angle and Spectrometric Coronagraph (LASCO) on board the Solar and Heliospheric Observatory (SOHO) were obtained from the NASA website at https://cdaw.gsfc.nasa.gov/CME_list/index.html. The SOHO LASCO CME catalog provides the speed and angular size estimates of all CMEs for the period from 1996 until 2016. The data of geomagnetic storms was obtained the website Laboratory of X-Ray Astronomy of the Sun, LPI website. The TESIS is a set of solar imaging instrument developed by the Lebedev Physical Institute of the Russian

Academy of Science and launched aboard the Russian spacecraft CORONAS-PHOTON in January 30, 2009. It shows the data from the last 3 days of magnetic storms with three indicators such as geomagnetic calm, geomagnetic disturbances, and geomagnetic storm. Additional data of geomagnetic storms from WDC for Geomagnetism, Kyoto were also collected for comparison.

4.4 Data Treatment

SunPy is a developing tool applied for processing and analysis of solar data by using the advantages of Python (Campos Rozo & Vargas Dominguez, 2014). The common functionality provided by the base ***Spectrogram*** class includes joining different time ranges and frequencies, performing frequency-dependent background subtraction, and convenient visualization and sampling of the data. The ***CallistoSpectrogram*** object retrieves spectrogram data in the time range specified. When the data is requested using the ***from_range ()*** function, the object merges all the downloaded files into a single spectrogram, across time and frequency (Mumford et al., 2015).

The SunPy was used to analyze the spectrogram image by reducing the unwanted signal or noise in the image which is in the form of noise. Otherwise, the spectrum gives an inaccurate reading of frequency and time (refer Appendix A for the coding). The example in Figure 4.2 demonstrates the radio spectrograms from the e-Callisto with the implemented background subtraction method. In order to remove the unwanted signal, an important thing that needs to considered is to ensure that the valuable signal is not removed, thus providing a quality data. The noise is reduced while maintaining its spectral characteristics. This problem can be overcome by adjusting the Vmin (can be varied from 0 to 5) to normalize the color.

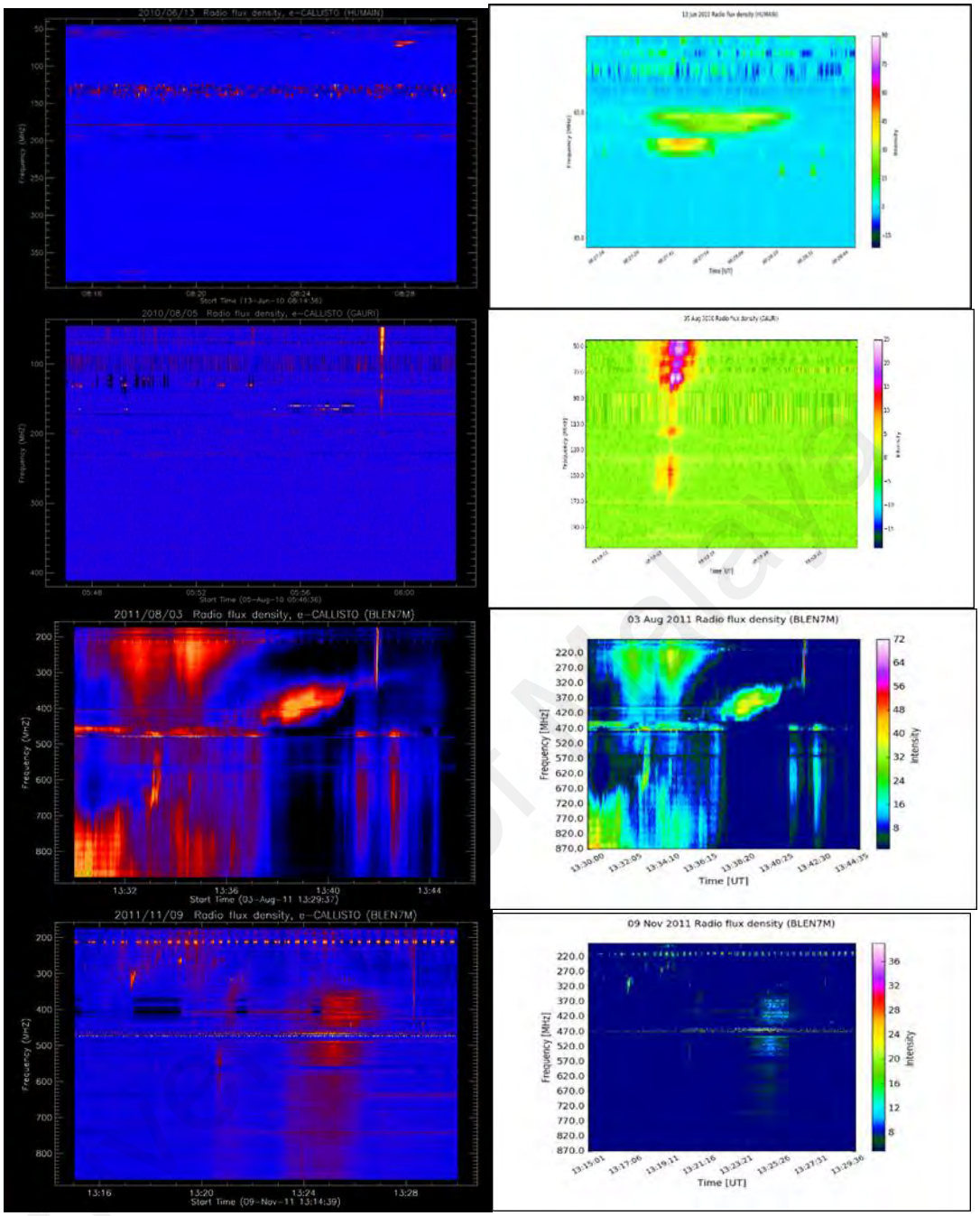

Figure 4.2: Left; The original spectrogram of solar radio burst. Right; A nicer image after reducing the noise using Sunpy by Python.

This software application was used to acquire a precise estimation of the frequency and time of solar radio bursts observed in this study. However, the data presented in the chapter on results and discussions were mainly from the primary spectrogram from CALLISTO.

CHAPTER 5: RESULTS AND DISCUSSION

5.1 Statistical Data

A statistical study of type III and type IV solar radio bursts were performed using the data from Compound Astronomical Low cost Low frequency Instrument for Spectroscopy and Transportable Observatory (CALLISTO) from 2006 until 2011. 2006 until 2011 were chosen to examine the properties of type III and type IV solar radio bursts because of the availability of complete archive list of solar radio bursts data provided by the e-CALLISTO website. Most importantly, it presents type III solar radio bursts which is mainly comrade with broadband continuum type IV solar radio bursts, which, in turn that are known to be well associated with geomagnetic storm.

The statistics of type III and type IV solar radio bursts were studied to see their frequency of occurrence within the specified years. As shown in Table 5.1, the occurrence of type III solar radio bursts is more frequent compared to the type IV solar radio bursts, with 320 and 37 events recorded respectively. These results confirm that type III solar radio bursts are the major burst that forms the maximum events in the phases of particle acceleration.

Table 5.1: Statistics of type III and type IV solar radio bursts from 2006 until 2011.

YEAR	SOLAR RADIO BURST TYPE IV	SOLAR RADIO BURST TYPE III
2006	1	15
2007	0	19
2008	3	10
2009	1	31
2010	8	45
2011	24	200
TOTAL	**37**	**320**

Note that, the events increase yearly as the number of CALLISTO sites also increases. As can be seen, the data of solar radio bursts increases drastically in 2011. This is because of an additional site of the CALLISTO spectrometer. Therefore, detection and monitoring of the Sun can be done with a longer period of observation as well as for 24 hours per days.

Comparatively, there are only a few detections of solar radio bursts in the 2006. Accordingly, in the beginning of this project, the installation of CALLISTO spectrometer have only 12 sites, and subsequently not having the 24 hours Sun monitoring. Other than that, both solar radio bursts rise from 2010 to 2011. This might be due to the solar activities that increases during that time, since 2006 until 2008 are at the minimum to maximum phase of the solar cycle.

5.1.1 Distribution of solar radio burst type III and type IV

The main purposed of this study was intended to see the influence of type III solar radio bursts on the type IV solar radio bursts that will lead to the formation of geomagnetic storm. However, keep in mind that this study will not focus on the solar cycle whether it happens at the solar minimum or solar maximum phases.

Table 5.2 presents the distribution of type IV solar radio bursts events associated with other types of solar radio bursts for 2006-2011. From 37 events of type IV solar radio bursts, 20 events were preceded by type III solar radio bursts. The other 22 events were followed by type III solar radio burst and the rest with other types and no burst detected. Type IV solar radio bursts was preceded by 20 bursts of type III solar radio bursts, 5 by DCIM, 2 from type II solar radio bursts, 5 from type I solar radio bursts and the rest (5) with no burst detected at all. Other than that, type IV solar radio bursts with 18 events was both preceded and followed by type III solar radio bursts.

Table 5.2: Distribution of solar radio burst type IV events associated with others solar radio bursts for 2006-2011.

	Type IV		
	Preceded	Followed	Both
Type III	20	22	18
Other Type	12	12	7
No burst detected	5	3	-
TOTAL	37		

From this Table 5.2, it appears that the occurrence of type IV solar radio bursts is mostly associated with type III solar radio bursts. As this study focuses only on type III solar radio bursts associated with type IV solar radio bursts, the presence of type III solar radio bursts is only included based on the duration not exceeding more than 24 hours before the type IV solar radio bursts occur.

Type III solar radio bursts emission that commences after a type IV solar radio burst was not the focus of in this statistical study. However, there were 22 events listed in the e-Calisto archive in which type III solar radio bursts are followed type IV solar radio bursts.

5.1.2 Classification of solar radio bursts type III and type IV

As a comparison, the classification was done by the presence or absence of an associated type III solar radio bursts. In order to examine their possible relation, the set of 37 events was divided into two groups with two classifications, one depending on the presence of type III solar radio bursts that preceded type IV solar radio bursts and the other on type IV solar radio bursts only (without the presence of type III solar radio bursts before the occurrence of type IV solar radio bursts). Figure 5.1 shows plot of k_p index, an index of geomagnetic variability, for each of the 37 events of the type IV solar radio bursts at 3-hour intervals.

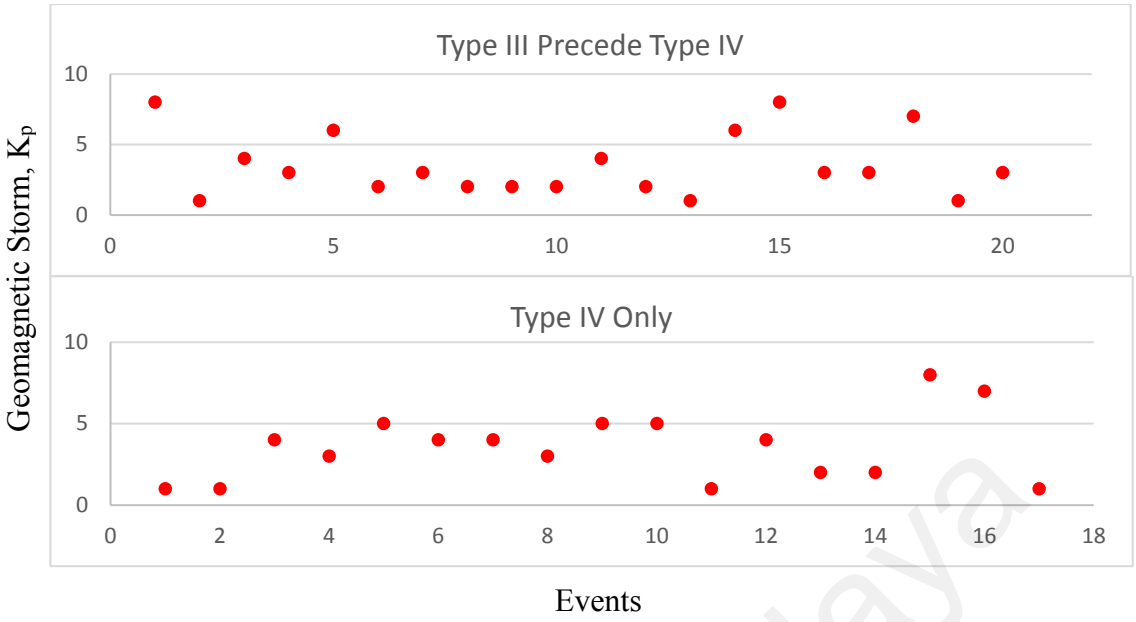

Figure 5.1: Distribution of geomagnetic storm activity as a function of events: (above) type III solar radio bursts preceding type IV solar radio bursts with 20 events; (below) type IV solar radio bursts only without type III solar radio bursts with 17 events.

Similar trends are clearly seen among both type IV solar radio bursts in the presence of type III solar radio bursts and type IV solar radio bursts only. With 20 events of type IV solar radio bursts being preceded by type III solar radio bursts, there are 5 events associated with great geomagnetic storms with k_p index of 6 to 8, 2 events with geomagnetic disturbance and the rest (13) events are geomagnetic calm with k_p index from 1 to 3. While, for type IV solar radio bursts only without the associated type III solar radio bursts, 5 events have geomagnetic storm of k_p index from 5 to 8, with three of them at 5 k_p index. 4 events of geomagnetic disturbances and 8 events of geomagnetic calm.

As can be seen, with the presence of the type III solar radio bursts before type IV solar radio bursts event, the association of geomagnetic storm was greater compared to type IV solar radio bursts only. Even though type IV solar radio bursts only also have a geomagnetic storm, but it occurs at the index of 5 and only two events at index of 7 and 8, compared to type IV solar radio bursts that has been preceded by type III solar radio bursts with its associated 6 to 8 k_p index.

This association between type III and type IV solar radio burst can be explained by the fact that both of these solar radio bursts are generated by fast electrons. The disturbance that causes the acceleration of type III solar radio bursts have high velocities and possibly either streams of electrons or fast transverse shock. The electrons which give rise to type IV solar radio bursts principally also have a similar velocity range (Thompson, 1962).

5.1.3 Association with solar flares, solar wind and active regions

Although not showing an outstanding difference in the presence and absence of type III solar radio bursts as shown in Figure 5.1, this might be due to some other factors. Among the factors that affect the geomagnetic storms are solar flares and solar wind. Table 6.3 compares the various categories of all type IV solar radio bursts events in the presence of type III solar radio bursts and type IV solar radio burst only with respect to powerful solar flares, great geomagnetic storm, speed of solar wind and from which active region the events was released.

As shown in Table 5.3, all type IV solar radio bursts storms are found to be associated with very large solar flares. Predominantly, solar radio bursts events are accompanied with solar flares (from classes C to M), producing major storms.

For type IV solar radio bursts events preceded by type III solar radio bursts, about half (9 events) of the events are found to be associated with major flares of X-class and M-class. It is clearly shown that 6 out of 9 events associated with great flares have sunspot that are directed towards the Earth and the rest are not Earth directed or near to east or west limb. However, it can be seen that only 2 events have high solar wind speed of more than 500 km/s. For type IV solar radio bursts only, the situation is reversed, showing that 10 events associated with powerful solar flare have a slower solar wind speed below than 500 km/s.

Table 5.3: Association of solar radio bursts events with solar flares, geomagnetic storm, solar wind and active region.

TYPE IV WITH TYPE III						TYPE IV ONLY				
No.	Date	Solar Flare	Geomagnetic Storm Index	Solar Wind, km/s	Active Region	Date	Solar Flare	Geomagnetic Storm Index	Solar Wind, km/s	Active Region
1	13-Dec-06	X3.4	8	645	930	2-Nov-08	Class B	1	401.2	1007
2	3-Nov-08	Class B	1	379.9	1007	11-Dec-08	Class B	1	418.1	1009
3	13-Feb-10	C9.6	4	308.2	1048	12-Feb-09	Class B	4	339.7	1012
4	13-Jun-10	M1.0	3	400.4	1079	12-Feb-10	M8.3	3	340.9	1046
5	1-Aug-10	C3.2	6	476.4	1092	16-Feb-11	M1.6	5	407	1158
6	5-Aug-10	C1.3	2	518.7	1093	3-Mar-11	C5.4	4	630.8	1164
7	14-Aug-10	C4.4	3	408.7	1099	7-Mar-11	M3.7	4	389.9	1164
8	18-Oct-10	C2.5	2	379.5	1112	30-May-11	C7.0	3	566.2	1226
9	19-Oct-10	C1.3	2	431.2	1112	2-Jun-11	C3.7	5	417.3	1226
10	22-Jan-11	C2.4	2	372.3	1149	7-Jun-11	M2.5	3	467.2	1226
11	14-Feb-11	M2.2	4	400.9	1158	29-Jun-11	Class B	1	339.1	1242
12	15-Feb-11	X2.2	2	460.2	1158	2-Aug-11	M1.4	4	405.8	1261
13	24-Feb-11	M3.5	1	325.2	1163	22-Sep-11	X1.4	2	405	1302
14	1-Mar-11	C6.0	6	621.8	1164	23-Sep-11	M1.9	2	373.4	1302
15	3-Aug-11	M6.0	8	356	1261	24-Sep-11	X1.9	8	326.3	1302
16	9-Aug-11	X6.9	3	551.5	1263	25-Sep-11	M7.4	7	347	1302
17	11-Aug-11	C6.2	3	413.6	1263	25-Dec-11	M4.0	1	368.8	1387
18	1-Oct-11	M1.2	7	532.7	1305					
19	9-Nov-11	M1.1	1	353.3	1343					
20	13-Nov-11	C2.6	3	366.7	1347					

Despite its association with great solar flares but still having a lower geomagnetic index, this might be due to which active region releases and the solar wind speed. Which part of solar disc must also be taken in consideration whether it was ejected from the sunspot that is directed to Earth or not. If it is not directed towards the Earth, the energy that disturb Earth's magnetic field is too small thus leading to a minor geomagnetic storm only. This is in comparison to other Earth-directed energies which is, of course, will give energy to the magnetic field.

This proves that, even though it has high solar flare ejected from the active region that is Earth-directed, but the solar wind speed is low thus, there is not enough energy to eject the electron into the interplanetary medium to disturb Earth's magnetosphere. Rapid speed winds bring geomagnetic storms while moderate speed winds bring quiet space weather.

Other than that, there also some events which has a slow solar wind speed but have higher geomagnetic storm index and great solar flare. This happens due to the accompanying CME that injects more energy into the magnetic field. The association of CME in producing geomagnetic storm will be discussed in selected events.

Generally, the occurrence of type IV solar radio bursts with geomagnetic storm have an outstanding relation. It was largely confirmed by the findings from this study (not shown in the table) where the 12 events of the great geomagnetic storm (indexes from 5-8) are associated with powerful flare. Out of 12 events, 3 events were C class flare and the remainder are M-class and X-class flare.

5.1.4 Parameters of type III and type IV solar radio bursts

The parameters of type III and type IV solar radio burst can be seen in Figure 5.2 and Figure 5.3 with the energy as a function of geomagnetic storm and frequency drift as a function of geomagnetic storm respectively.

Figure 5.2 obviously shows the energy of type III solar radio bursts has lower energies than type IV solar radio bursts as presented on 5 August 2010, 14 August 2010,18 October 2010, 22 January 201115 February 2011, 24 February 2011, 9 November 2011 and 13 November 2011, with the geomagnetic storm observed are below 4 k_p index. This indicates that the energy from type III solar radio bursts is necessary in producing higher level of geomagnetic storm. Event thought type IV solar radio burst have high energy, it not enough to produce a great geomagnetic storm.

Other than that, there is a special case where the type III solar radio bursts have low energy, but high geomagnetic storm as shown on 1 August 2010, 1 March 2011, 3 August 2011 and 1 October 2011. It might be due to the type III solar radio bursts not requiring many electrons in a beam to produce a detectable type III solar radio burst. This is because the plasma emission mechanism is very efficient at converting a small amount of free energy in an electron velocity distribution into electromagnetic emission.

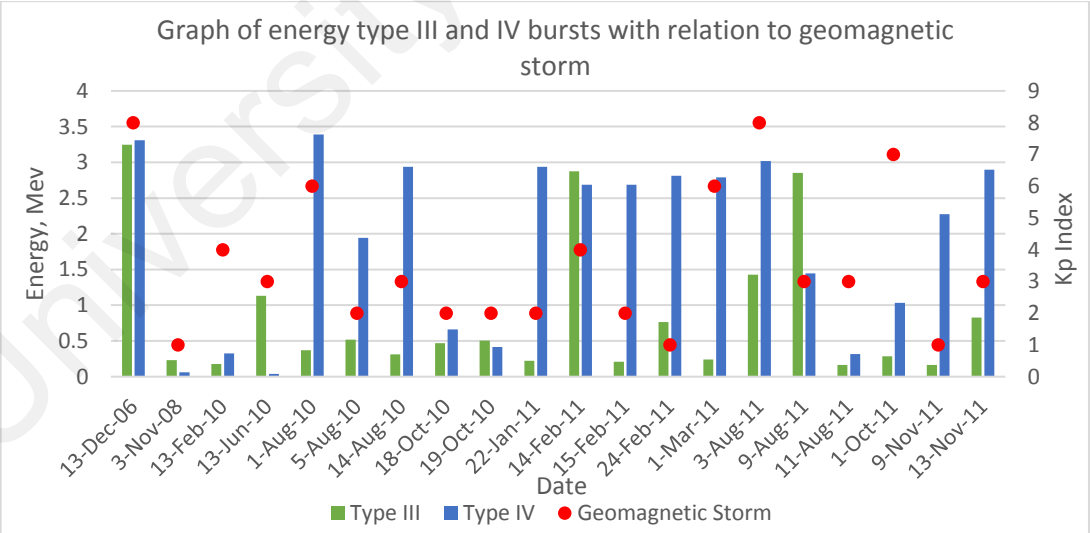

Figure 5.2: Distribution of energy type III and type IV solar radio bursts.

It is well known that type III solar radio bursts have a high frequency drift rate. This clearly can be seen in Figure 5.3, where the type III solar radio bursts dominate the graph. The high frequency drift of type III solar radio burst is due to how fast the electron travels in the interplanetary medium. That will help in ejected the energy. However, there are a special case on 1 March 2011 and 1 October 2011 where the frequency drift of type IV solar radio bursts is higher than type III solar radio bursts.

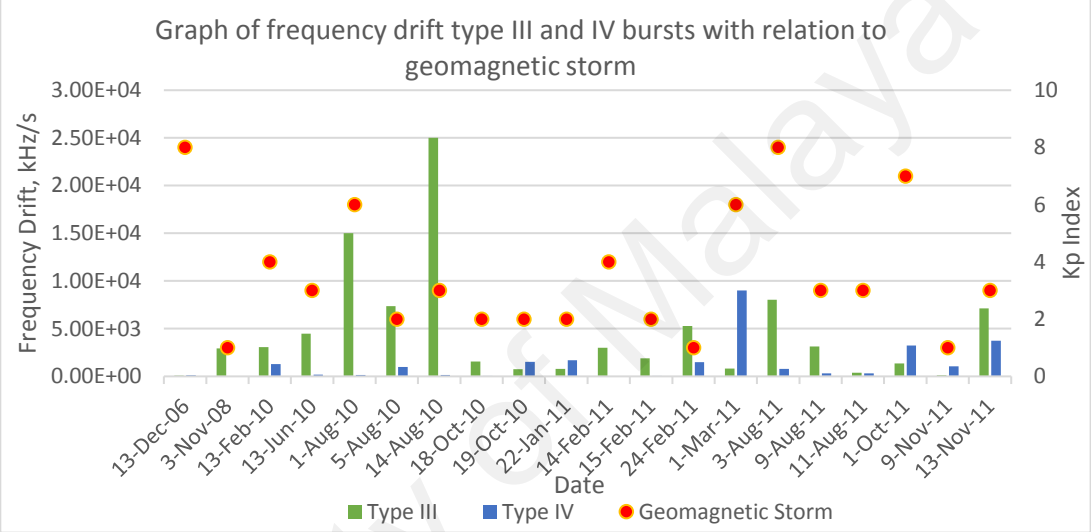

Figure 5.3: Distributions of frequency drift in type III and type IV solar radio bursts.

The findings from these two Figures shows the relationship between energy and frequency drift of the solar radio bursts. It can be seen, when the energy of solar radio bursts is high, the drift rate is low. This is because the energy from the Sun flows out with low velocity, thus having many energy levels. Conversely, when drift rate is high, it is ejected at high speed from the corona and energy dispersed into the interplanetary medium. The energy is also low because the density of coronal plasma decreases with distance from the Sun.

5.2 Selected Data: A Case Study of Solar Radio Burst Type IV and Type III

The events were selected on the basis that the spectrum distinctly shows type III solar radio bursts were observed before the onset of type IV solar radio bursts in the years 2006-2015. Furthermore, in order to see the relationship of type III solar radio burst with type IV solar radio burst, the events were presented by showing that the type IV solar radio burst was both preceded and followed by a type III solar radio burst. Other than that, also included is the event where the type IV solar radio burst is followed by a type III solar radio burst to see whether it gives any impact to the solar activity.

5.2.1 Observations on 13th December 2006

Figure 5.4 shows a fast drift type III solar radio burst which was followed by broadband smooth continuum type IV solar radio burst. At 0935 UT there was a strong single type III solar radio burst starting at 60 MHz and lasting for 2 seconds. Other than that, there are contributions from a second storm type III solar radio burst that starts at 0224 UT and detectable above 100 MHz and lasting for 2 hours. In addition to the storm type III solar radio burst, these were followed by flare continua type IV solar radio burst at 0227-0230 UT from 150-300 MHz. Furthermore, a stationary emission of type IV solar radio burst detected was between 0230 UT and 0440 UT in the frequency range 150-900 MHz.

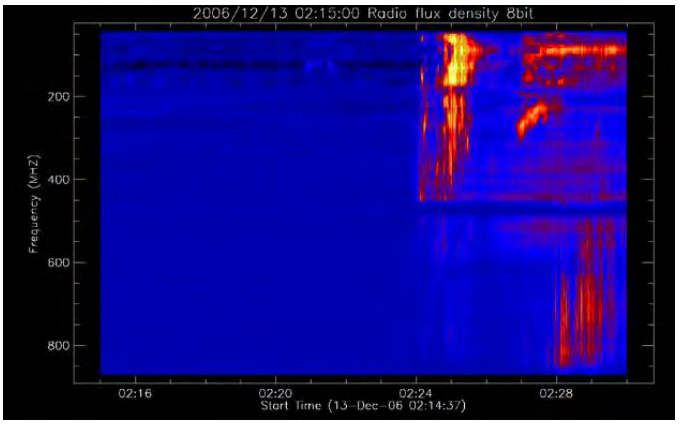

Figure 5.4: A single type III solar radio burst followed with flare continua type IV solar radio burst.

These bursts are accomplice with the great solar flare type X 3.4 class which is registered as the larger ones. The flare lasted from 0240 UT to 0810 UT along with one active region during this event. Moreover, this event was associated with the severe geomagnetic storm observed on 14th December 2006. It occurs 24 hours after the emission of solar radio burst type III and type IV events. It was reported with 2 moderates (level G2), strong (level G3) and severe storm (level G4) with k_p index of 6,7 and 8 respectively as shown in Figure 5.5.

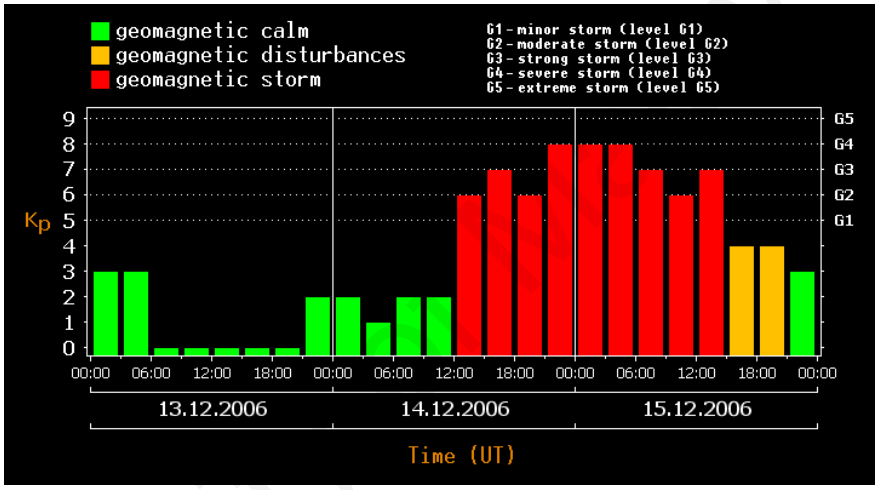

Figure 5.5: The fluctuation of geomagnetic storm arises from the solar events on 13th December 2006.

Besides that, there is a halo CME travelling with a speed 1774 km/s onset at 02:25:03 UT with the first appearance at 02:54:04 UT. It was confirmed, the one responsible for hurling this giant CME is the sunspot AR 930. The solar wind speed during this event is 645.0 km/s with proton density of 0.6/cm3 and the sunspot number is 27. As reported by the spaceweather.com website, it was predicted that satellites may experience a temporary malfunction and reboots, but not harmful to the astronauts. It has been believed, that the type III and type IV solar radio burst is well associated with the development of solar flares. Relies upon this fact, Figure 5.6 presents type III and type IV solar radio burst commonly seen in the impulsive phase of the solar flare. The solar flare begins at 02:14:00

UT with the maximum peak at 02:40:00 UT, with the appearance of type III solar radio burst at 0224 UT, followed by type IV solar radio burst at 0227 UT.

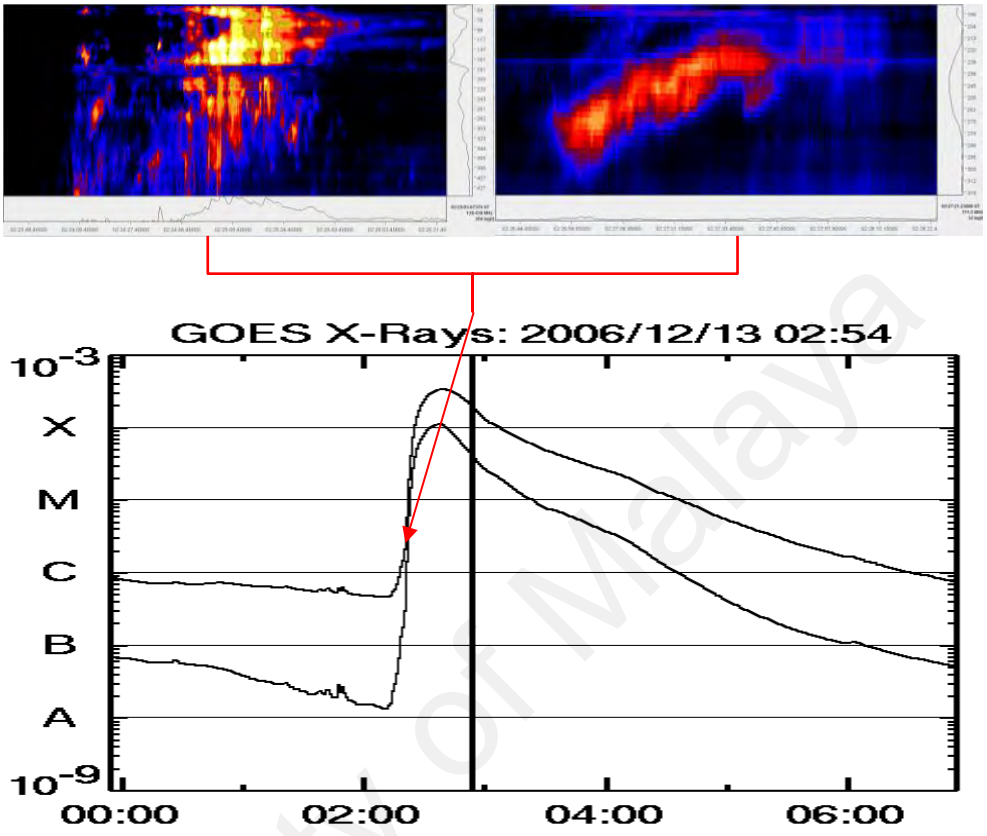

Figure 5.6: The variability of big solar flare hurled on 13th December 2006. It appears that type III and type IV solar radio burst occur at the time of impulsive solar flare.

The type III and type IV solar radio burst are the radio signatures of the phases of particle acceleration. It is apparent that the phases dominate in flares when the particle escape into the interplanetary medium. Also, it been long known that the beam electrons of type III solar radio burst are a producer of electrostatic Langmuir waves via the bump-in-tail instability. Furthermore, type III solar radio burst lasted for two hours. This might be an indicator that type III solar radio burst are also associated with the decay phase of the solar flare. It has long been known that the solar flare and CME both lie in the same layer of solar atmosphere, proved by these events when CME started 11 minutes after the solar flare began.

5.2.2 Observation on 3rd November 2008

Figure 5.7 shows data for the weaker single type III solar radio burst onset at 0807 UT that lasted for 3 seconds at frequency range 50-100 MHz. After 17 minutes, the type III solar radio burst was followed by a type IV solar radio burst from 0824-0830 UT at high frequency range starting from 1410 until 1425 MHz. Further five single type III solar radio bursts detected at 0025 UT, 0103 UT, 0829 UT, 0923 UT and 1459 UT, all of which occurred for a second and before the start of the solar flare. There was a reported solar flare class B and calm geomagnetic storm with 1 k_p index.

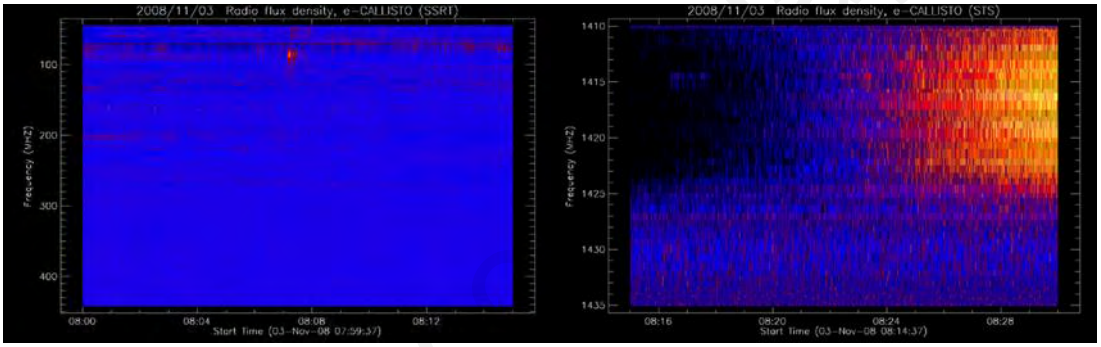

Figure 5.7: A single type III solar radio burst was followed by type IV solar radio burst.

The CME was reported with much slower speed of 433 km/s appearing at 05:54:04 and onset at 04:55:51 UT. There is one Active Region during this event and was considered a member of new solar cycle 24. As reported by the spaceweather website, this is the fourth new-cycle sunspot in the past month after a year almost no sunspots. During the solar minimum (year of 2008), the sunspot number is only 17 because the Sun in the quiet phase. As expected from the above parameter, the effect of solar activity towards Earth's magnetic field is low. This is because the type III solar radio burst is the thermal emission burst which is produces low energy. Even though this event was released from sunspot AR 1007 which is on the Earth-facing side of the Sun, but the speed of the CME is very slow to harbor the plasma into the interplanetary space.

5.2.3 Observation on 1st August 2010

The solar radio burst associated with solar activities event of 1st August 2010 are shown in Figure 5.8. At 0914-0923 UT, there are moving type IV solar radio burst from 48-410MHz. Coupled with this event, a stationary broadband continuum with fine structure type IV solar radio burst from frequency range 180-880 MHz which is lasted for two hours from 0754-1036 UT. This type IV solar radio burst was preceded by seven single type III solar radio bursts occurring above 50 MHz at 0432 UT for a second. Other than that, the type IV solar radio burst was also followed by group of type III solar radio burst during the interval 1415-1417 UT, 1146-1148 UT and 1548-1550 UT with the frequency range between 170-400 MHz.

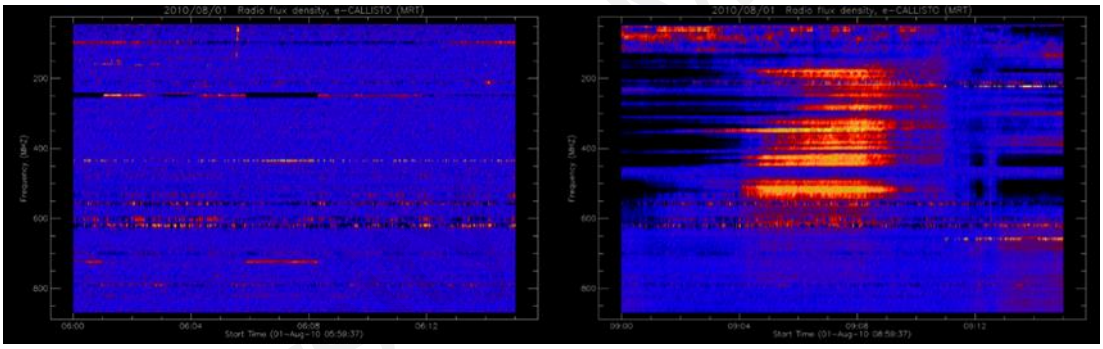

Figure 5.8: A moving, and stationary burst type IV was preceded and followed by type III single burst.

There are 3 Active Regions during this event with 12 sunspot numbers. Moreover, there was a solar flare C3.2 class at 07:55 UT blasting from sunspot AR 1092. In addition, an enormous magnetic filament stretching across the Sun's northern hemisphere erupted at about the same time as solar flare onset. The maximum peak of the solar flare is 08:26 UT and ended at 09:35 UT. The magnetic storm associated with this complex radio activity was witnessed about 48 hours later with a k_p index level of G1 (minor) and G2 (moderate) occurring from 1800 UT to 2400 UT are shown in Figure 5.9.

A CME produced by this event headed directly towards the Earth as recorded by SOHO. It was travelling slowly with speed of 127 km/s, appearing at 00:30:05 and onset at 21:28:51 UT with mass 7.20×10^{13} g.

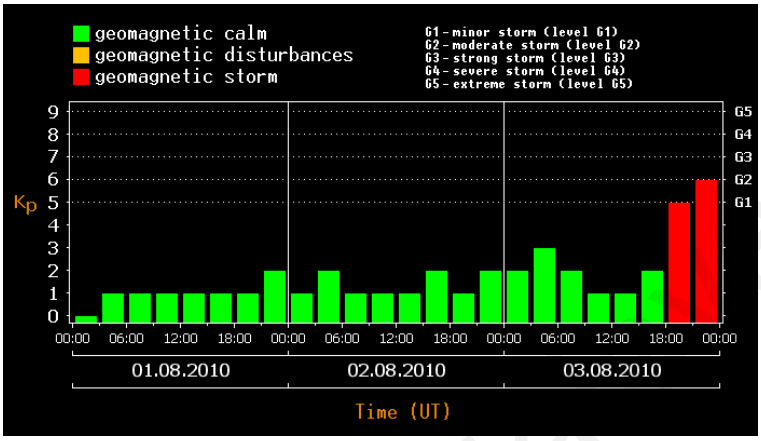

Figure 5.9: The geomagnetic storm on 3th August 2010. Arise from the impact of solar events on 1st August 2010.

These events show a weak solar radio burst even as well as solar flare and CME. Based on the previous statement, supposedly the energy that impacted on Earth's magnetosphere is low because only a single type III solar radio burst was present before type IV solar radio burst. Besides, coupled with this solar radio burst events are C class solar flare which is registered as a weaker one. But on the contrary, the geomagnetic storm is reportedly high during these solar events. This can be explained by referring to Figure 5.10. It shows a huge coronal hole stretching on the solar surface and Earth-facing side of the Sun. This coronal hole erupted a filament at almost the same time as the solar flare. Despite the ~400,000 km distance between coronal hole and sunspot AR 1092, they are probably connected by long-range magnetic fields. This coronal hole is responsible for releasing the solar wind towards the Earth, even though the recorded velocity is low with only 476.4 km/s. It may give additional impact on Earth's magnetic field instead of just from the CME and solar flare.

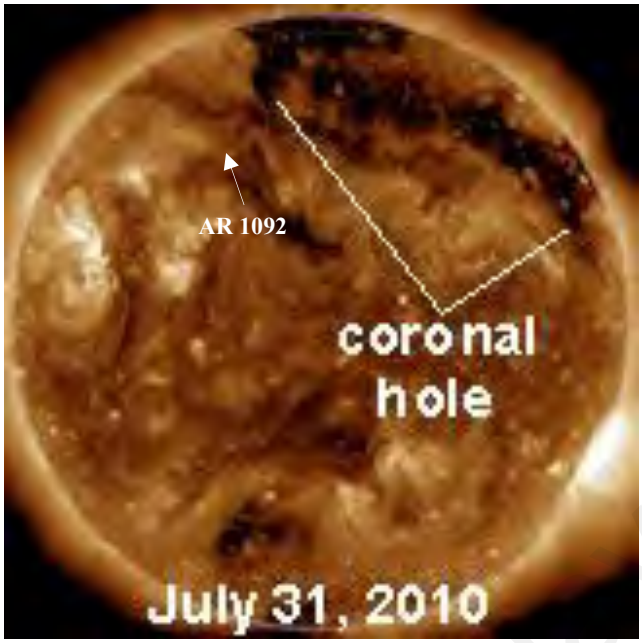

Figure 5.10: Solar wind stream on 1st August 2010 was flowing from this coronal hole.

5.2.4 Observation on 3rd August 2011

The 3 August 2011 solar radio burst event shows a type IV solar radio burst was preceded and followed by type III solar radio burst. A group of type III solar radio burst at 0817-0818 UT from the frequency range of 60-70 MHz that was detected by the BIR station. Two hours later, a smooth continuum moving type IV solar radio burst with strong structure appear at 1030-1349 UT at the frequency range of 160-900 MHz that was detected from BLEN7M, HUMAIN, INPE and MRO stations. This type IV solar radio burst then was followed by single type III solar radio burst which occurs above 30-700 MHz at 1200-1904 UT. A single type III solar radio burst was recorded at BIR, BLEN7M, and OOTY stations. As can be seen in Figure 5.11, there are strong storm type III solar radio burst starting at frequency range from 150-900 MHz at 1323 UT – 1337 UT, which is was preceded type IV solar radio burst by split of seconds.

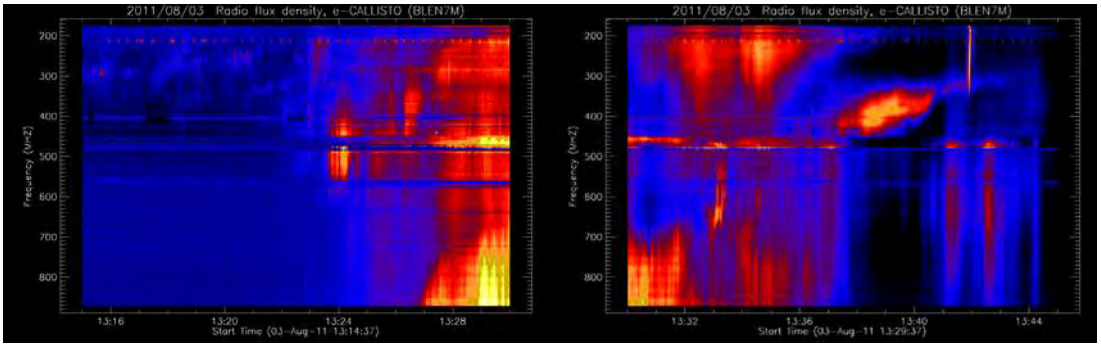

Figure 5.11: The spectrogram showing of group type III solar radio burst, moving type IV and single type III solar radio burst from BLEN7M.

There are 5 Active Regions recorded during this event with 98 sunspots number. The event was associated with M6 class of solar flare erupting from the AR 1261 active region. The active region during this day faces towards Earth, the same as the coronal hole that streams the solar wind with the speed of 356 km/s. Figure 5.12 show the variability of the solar flare that was recorded from TESIS laboratory of X-ray astronomy of the Sun, LPI RAS, Russia. This solar X-ray began to release energy from 13:17 UT until 14:10 UT with the maximum peak at 13:48 UT. The type IV solar radio burst ends almost exactly at the time of the soft X-ray peak at 1349 UT, regarded as the time at which energy release in the flare ends.

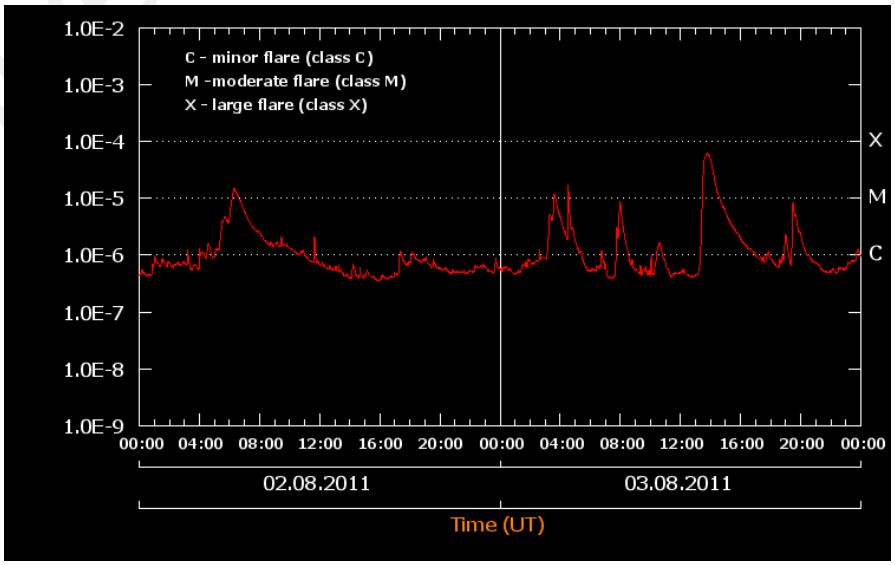

Figure 5.12: The solar flare M class on 3rd August 2011.

In addition, it a CME was detected travelling towards the Earth with a speed of 296 km/s and reached it about 48 hours later. In addition, severe geomagnetic storm level G4 and strong storm level G3 were recorded from 1800 UT to 0000 UT on 5 August 2011, as shown in Figure 5.13. Moreover, the listening station above the Arctic Circle in Norway reported ionospheric waves and VHF radio noise during these events.

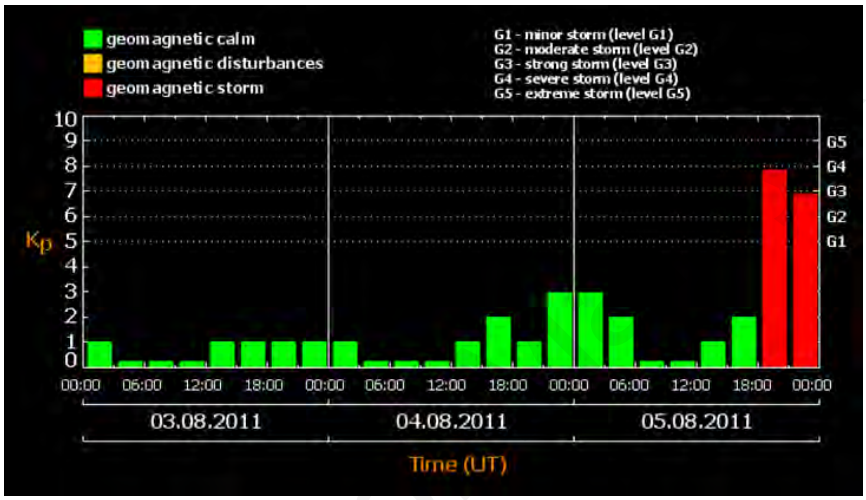

Figure 5.13: The geomagnetic storm on 5th August 2011.

A very positive relation was found between type III and type IV solar radio burst. A group of strong storm type III solar radio burst were separated by split seconds before the emission of type IV solar radio burst. Strong storm type III solar radio burst reflects a strong energy release by the intense solar flare. Since it occurs a couple seconds before the occurrence of type IV solar radio burst, it obviously provides some energy to the type IV solar radio burst.

Note that, these events also associated with CME that gives extra impact to the Earth's magnetic field. It reaches the Earth 48 hours after the commencement of solar events because the speed that brought this energy is low, both from the CME and solar wind.

5.2.5 Observation on 7th March 2012

To further investigate the relationship between type III and type IV solar radio burst with solar geomagnetic storm, the data on 7th March 2012 were examined as shown in Figure 5.14. For these events, the type IV solar radio burst was preceded and followed by type III solar radio burst. There is a strong group of type III solar radio burst detected at 0112 UT-0117 UT from the frequency range 170-800 MHz before the occurrence of the type IV solar radio burst. At 00:18:58 UT there was a strong moving type IV solar radio burst that started at 20 MHZ and then continue with stationary type IV solar radio burst at 01:01:37 UT and lasted for about one hour. This type IV solar radio burst was followed by four single types III solar radio bursts at 0503-0504 UT, 0754-0755 UT, 1044 UT and 1413 UT all of which starting at frequency range 50-100 MHz, 10-100 MHz, 170-280 MHz and 170-300 MHz respectively.

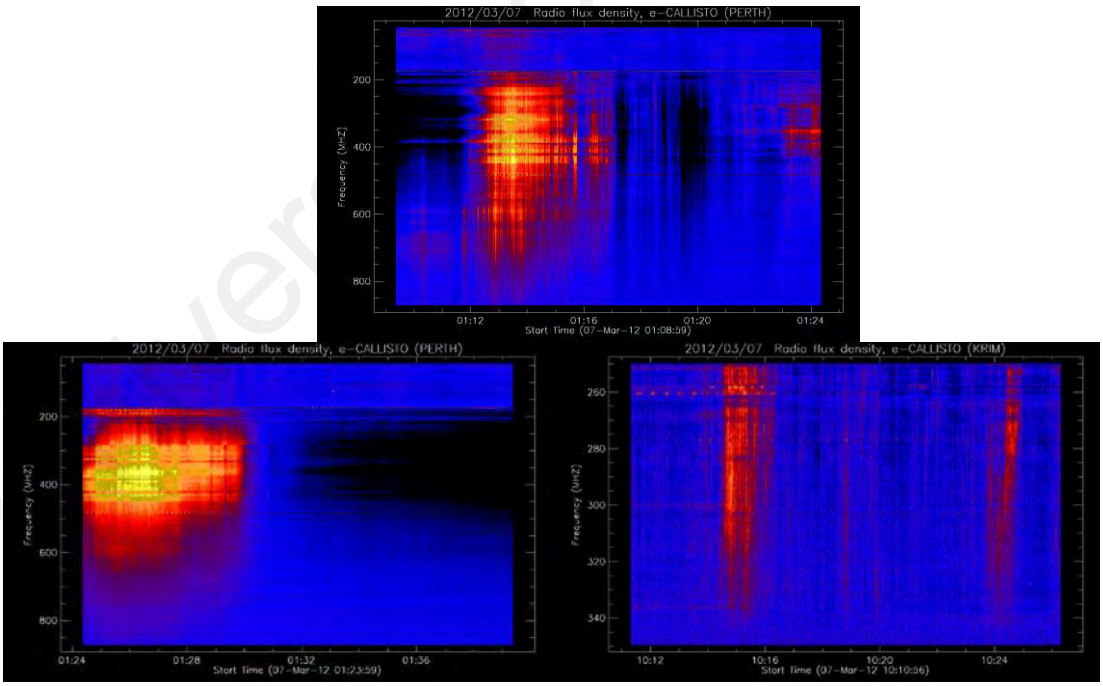

Figure 5.14: Strong moving type IV was following by single type III bursts.

However, there is a contribution from two groups of type III solar radio burst during the intervals 0800-0805 UT and 1547-1549 UT. The first one was in the frequency range 40-100 MHz and the second in the frequency range of 75-90 MHz. Besides, the storm type III solar radio burst was reported from 0948-1056 UT in the frequency range 250-400 MHz. In addition to this strong radio burst, this event also associated with X5.4 class flare blasting from AR1429 (Figure 5.15), being registered as a strong one. It was recorded that this flare started at 00:02:00 UT with the maximum peak observed at 00:24:00 UT and stopped at 00:40:00 UT.

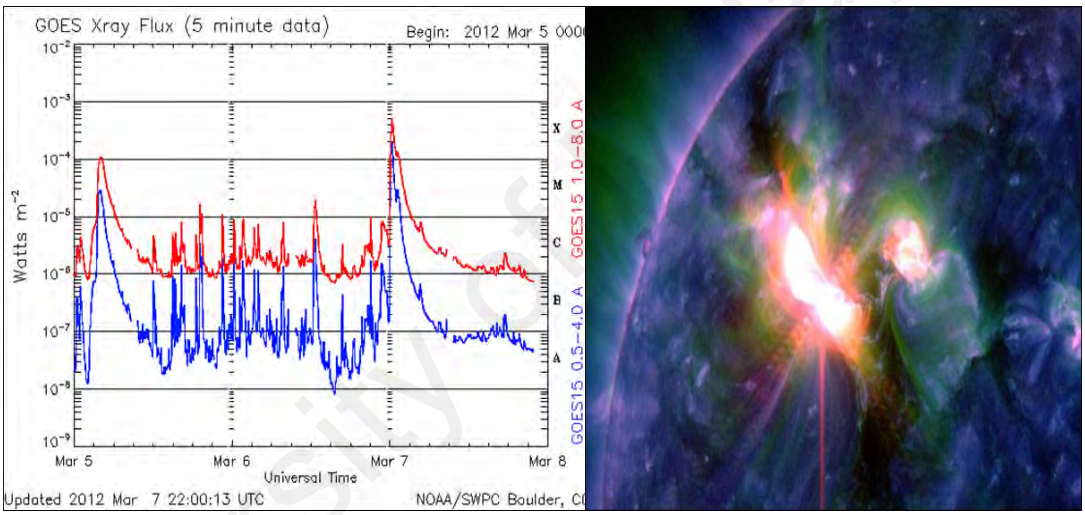

Figure 5.15: The variability of solar flare (left) and active region that propelled the CME (right) on 7th March 2012.

The halo CME has a speed of 1825 km/s, onset at 00:56:30 UT with first appearance at 01:30:24 UT. The mass was 1.40e+16 gram. There are 6 Active Regions during this event. Along with these events, they are associated geomagnetic storm occurred on 9th March 2012, with storm level G3 (strong storm) and G2 (moderate storm) as shown in Figure 5.16.

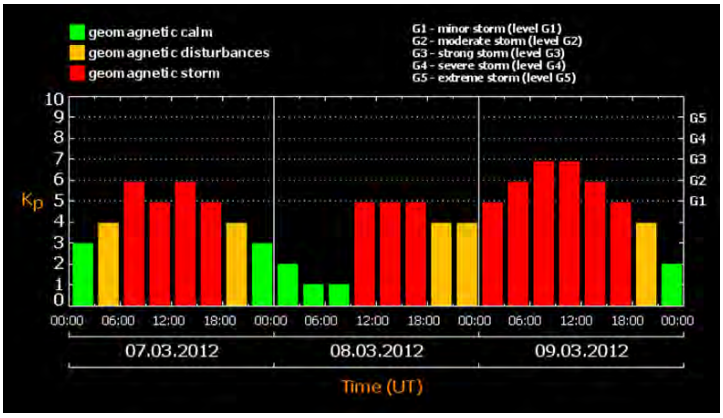

Figure 5.16: The variability of magnetic storm on 9th March 2012.

This is an interesting solar event to study their relationship with geomagnetic storm. This event presents a strong evidence of type III solar radio burst providing energy to the type IV solar radio burst thus leading to the commencement of geomagnetic storm. A careful observation on strong group type III solar radio burst has successfully recognized a nice complex radio burst event that shows a combination of type III and type IV solar radio burst. It is clearly showing that type III and type IV solar radio burst occur at the same time from 0112-0117 UT. Type IV solar radio burst were observed at frequency range of 200-450 MHZ while type III solar radio burst continue from 450-900 MHz as shown in Figure 5.17.

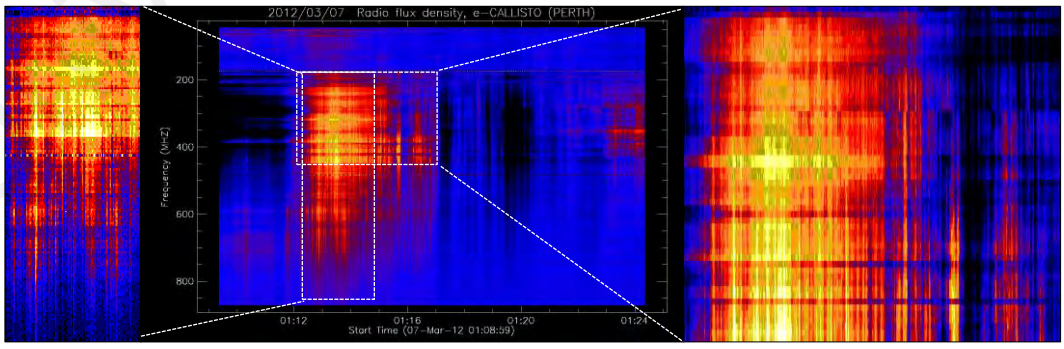

Figure 5.17: A close looked of the complex combination type III (left) and type IV (right) solar radio burst.

This may be an indicator of the associated CME during this event as these bursts appear a few seconds after the CME onset. It could happen because the emission for type III solar radio burst at the fundamental are believed to be cause by the interaction of Langmuir waves. the Langmuir waves are assumed to arise from excitation by shockwave (D. A. Gurnett, 1995). The disturbance which gives rise to type III solar radio bursts have high velocities and may be either an electron stream or transverse shock. While, the electrons which give rise to type IV solar radio bursts principally have a similar velocity range.

Moreover, the situation for geomagnetic storm is expected to be based on the powerful solar flare that occurred on this date. This is due to the intense flare that aggressively blasts particles and radiation into the interplanetary region. The energetic particles were emitting at meter and decameter wavelengths and can be detected as a solar radio burst by the process of bremsstrahlung radiation. In addition, the contribution of the halo CME ejected an enormous amount of charged particles at a very high speed also effects the measurement. Thus, a lot of the particles cross the magnetic field of the Earth and consequently produce high levels of geomagnetic storm.

5.2.6 Observation on 15th March 2013

Powerful stationary type IV solar radio burst was detected from the CALLISTO stations at ALMATY, BLEN7M, DARO, GAURI, HUMAIN and MRO. The duration of this burst which started at 0626-0900 UT lasted for two hours at the 180-900 MHz frequency range. After five hours, again BLEN7M station was detected a single type III solar radio burst with a frequency range of 200-400 MHz at 1404 UT. This type III solar radio burst lasted for 3 seconds. Figure 5.18 shows a stationary type IV solar radio burst followed by a single type III solar radio burst.

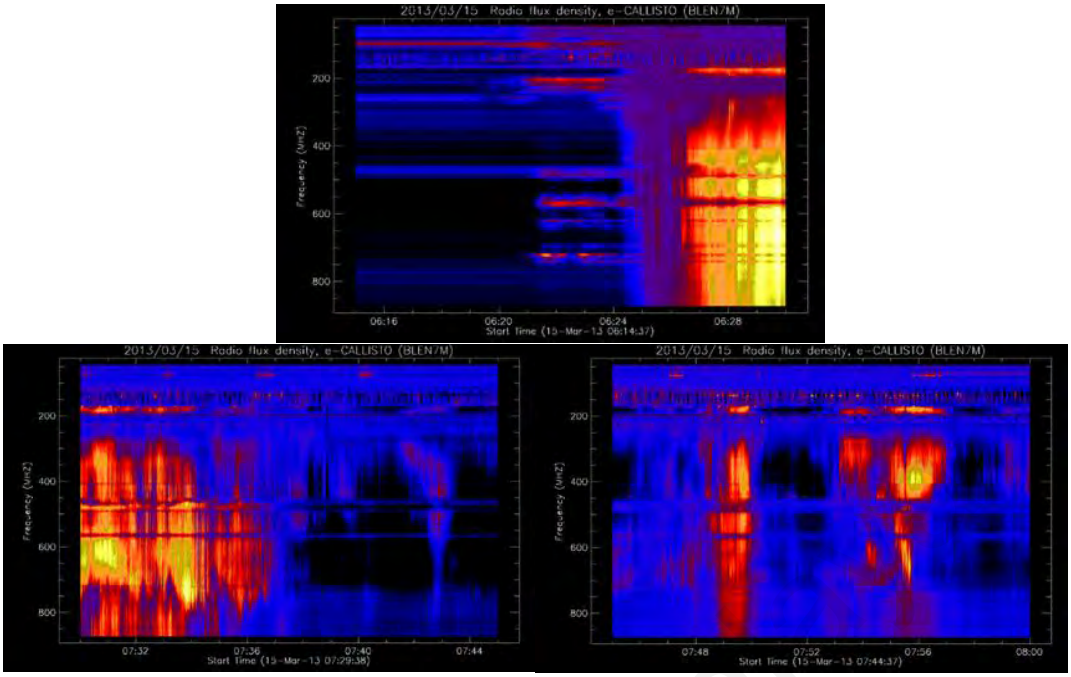

Figure 5.18: Stationary type IV solar radio burst followed by a single type III solar radio burst.

During this event, there are 9 Active Regions with sunspot number up to 133. The radio Sun recorded on this day is 10.7 cm flux with 123 sfu. The speed of solar wind is 444.5 km/s with proton density of 1.9 protons/cm^3 in the solar corona. The solar wind flows from the coronal holes as presented in Figure 5.19 and reached Earth's magnetic field on 17th March 2013. As can be seen, these giant coronal holes are facing directly toward Earth. There is no doubt a big impact on the Earth's magnetic field happened.

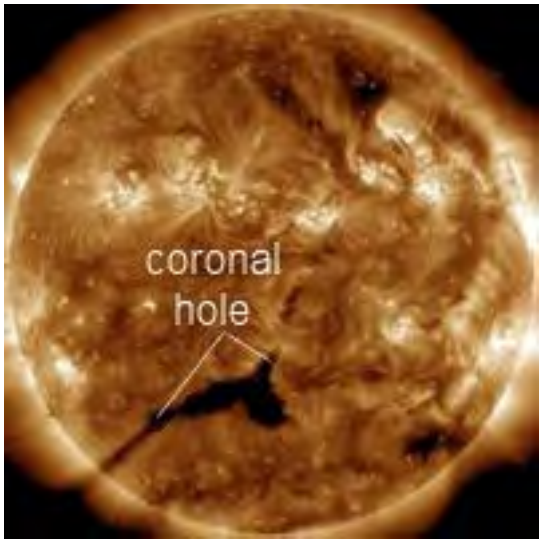

Figure 5.19: Coronal holes that flowing the solar wind on 15th March 2013.

A class of the M 1.1 solar flare was observed in X-ray region, with peak at 06:58:00 UT that began from 05:46:00 UT and stopped at 08:35:00 UT. Subsequently, the halo CME erupted at speed of 1063 km/s with the first appearance on the solar disc at 07:12:05 UT and first onset at 06:42:16 UT. The expanding cloud of CME and the variability of solar flare are shown in Figure 5.20. It was reported a magnetic filament twisting around sunspot AR1692 are believed the one responsible to blast a CME.

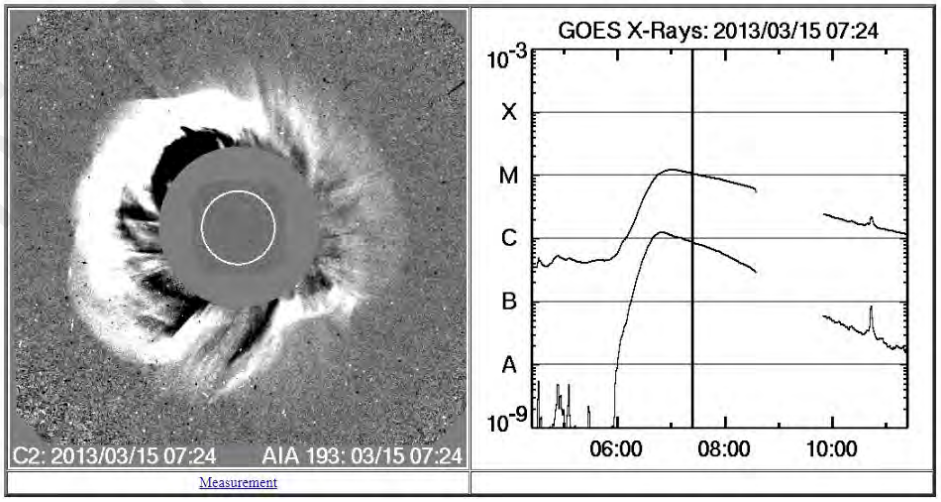

Figure 5.20: The halo CME cloud and the solar flare on 15th March 2013.

Coupled with the CME, the association of geomagnetic storm with level G2 (moderate) and G1 (minor) was observed two days later. The k_p index level of the geomagnetic storm was shown in Figure 5.21.

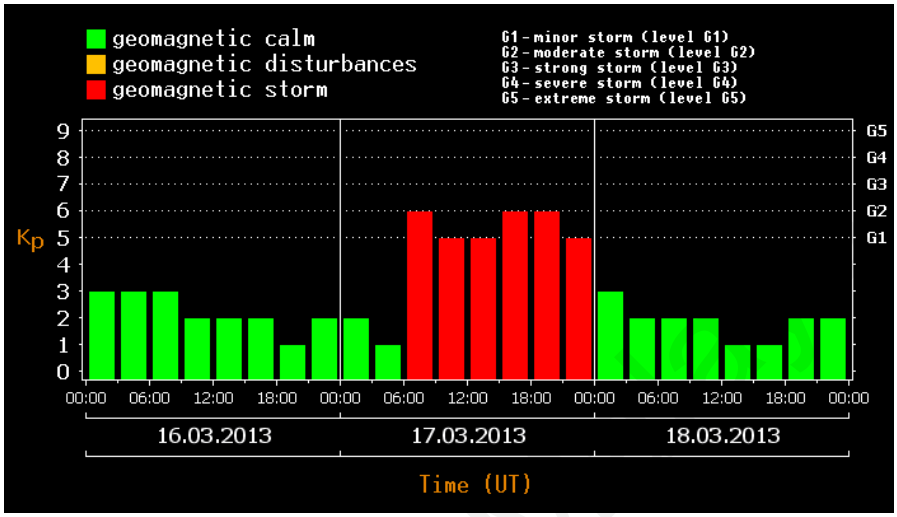

Figure 5.21: The geomagnetic storm on 17th of March 2013 that was delivered from CME events on 15th March 2013.

These solar radio events are a good example to show that the onset of type III solar radio burst after the occurrence of type IV solar radio burst but not giving any effect to the geomagnetic storm level. Even though it has a strong emission of type IV solar radio burst, it means nothing without the presence of type III solar radio burst before the type IV solar radio burst occurs. The plasma cloud that was ejected from the halo CME headed directly towards the Earth. For this reason, the CME is solely responsible for contributing towards the rise of geomagnetic storm for the solar events on 15th March 2013.

5.2.7 Observation on 10th September 2014

Figure 5.22 shows the type III and type IV solar radio burst using the data from DARO-HF and BIR stations on the 10th September 2014. Type III solar radio burst is seen occurring from 110-370 MHz at 1727 UT-1745UT. After a few seconds, a smooth continuum type IV solar radio burst was observed from 135-390MHz at 17:27 UT. This feature was associated with the decay phase of the solar flares.

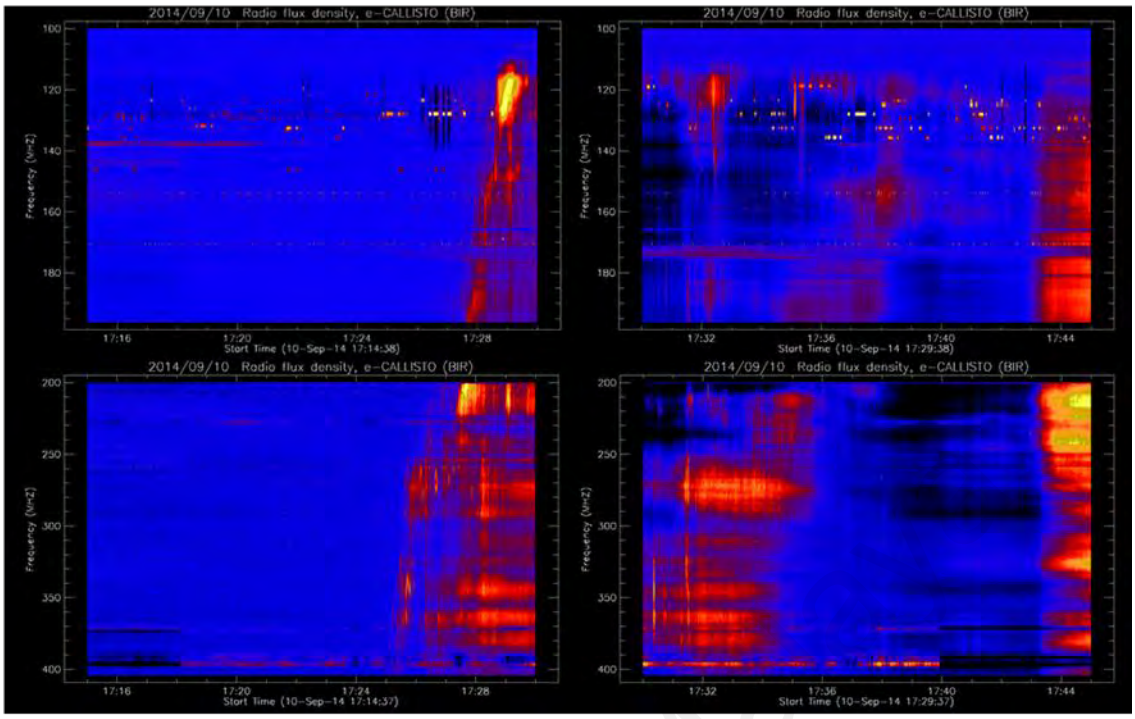

Figure 5.22: A single solar radio burst type III followed by type IV burst between 17:27 until 17:45 measured over a frequency range of 135MHz to 390MHz.

In addition to type III and type IV solar radio bursts, there were also type II solar radio burst reported during the interval 1728-1739 UT as shown in Figure 5.23. Based on the observation, it was found that type II solar radio burst with both fundamental and second harmonic band structure and splitting of each into two traces formed at 17:28 to 17:39 UT with high intensity. This slow drift herring bones structure occurred from 24-54 MHz and is an indicator of in the early rise of the impulsive phase of the solar flare.

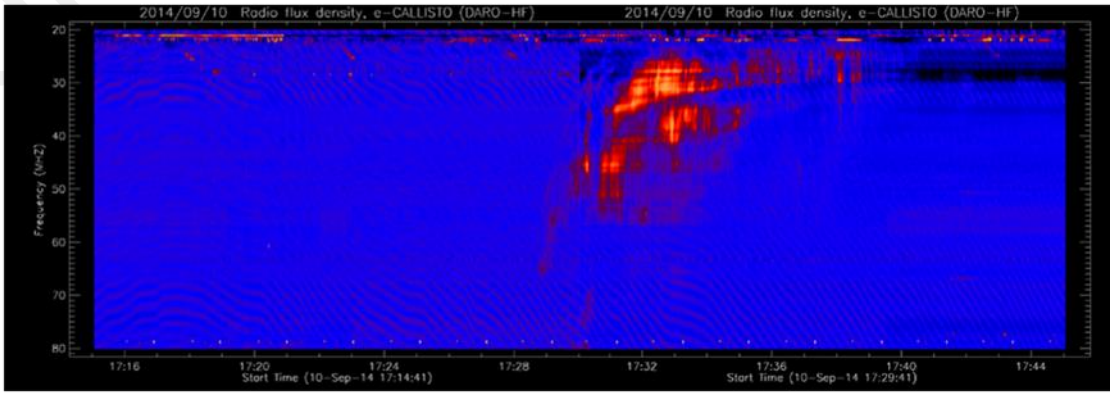

Figure 5.23: Type II burst with herring bones feature at 24-54 MHz from 17:28 – 17:39 UT.

Figure 5.24 shows the variability of the solar flare from the Solar Weather Prediction Center (SWPC) by National Oceanic Atmospheric Administration (NOAA). The sun storm occurred just after 1721 UT until 1820 UT with the maximum peak at 1745 UT and registered as a class X 1.6 solar flare which is one of the strongest types of solar flares possible. The huge solar flare erupted from the giant sunspot AR2158 and it stretches across 420 million of shares of the solar hemisphere. From this sunspot, it triggers a massive explosion of solar plasma known as coronal mass ejection as shown in Figure 5.25.

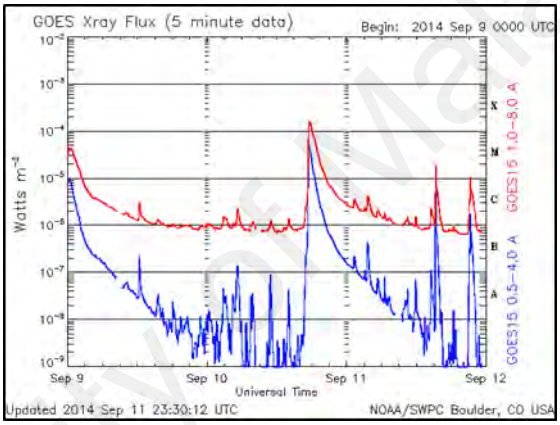

Figure 5.24: Solar flare during 10th September 2014.

A halo CMEs was ejected from AR2158 travelling with a speed of 1267 km/s directed towards the Earth. With this speed, it was expected to hit Earth's magnetosphere within 32 hours travelling from Sun to Earth. Accordingly, it was reported by Space Weather Web Site on 11th September 2014, a storm warning of a pair of CMEs that are heading toward the Earth from the solar storm that clouds were launched on 10th September 2014 by strong explosions in the magnetic canopy of sunspot AR2158. Furthermore, it also disrupts HF radio communication for more than half an hour. With a flash of ultraviolet radiation from the explosion, it also ionized the upper layers of Earth's atmosphere. It happened because the sunspots AR2157 and AR2158 have an unstable magnetic field that harbor energy for strong explosions.

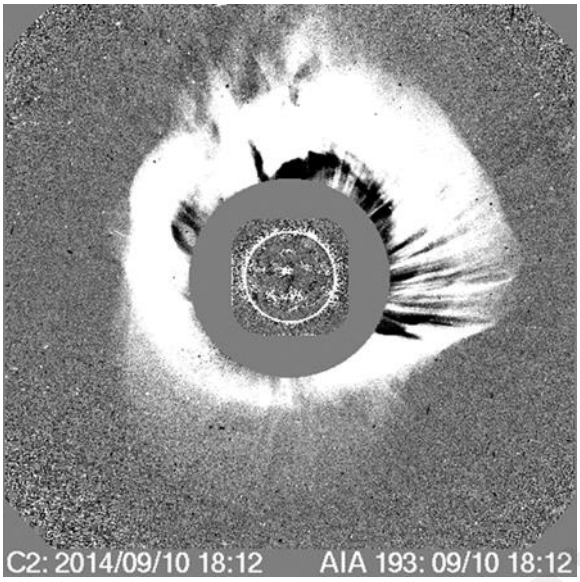

Figure 5.25: A halo CME coronagraph was recorded by SOHO LASCO C2 on 10th September 2014 at 18:12 UT.

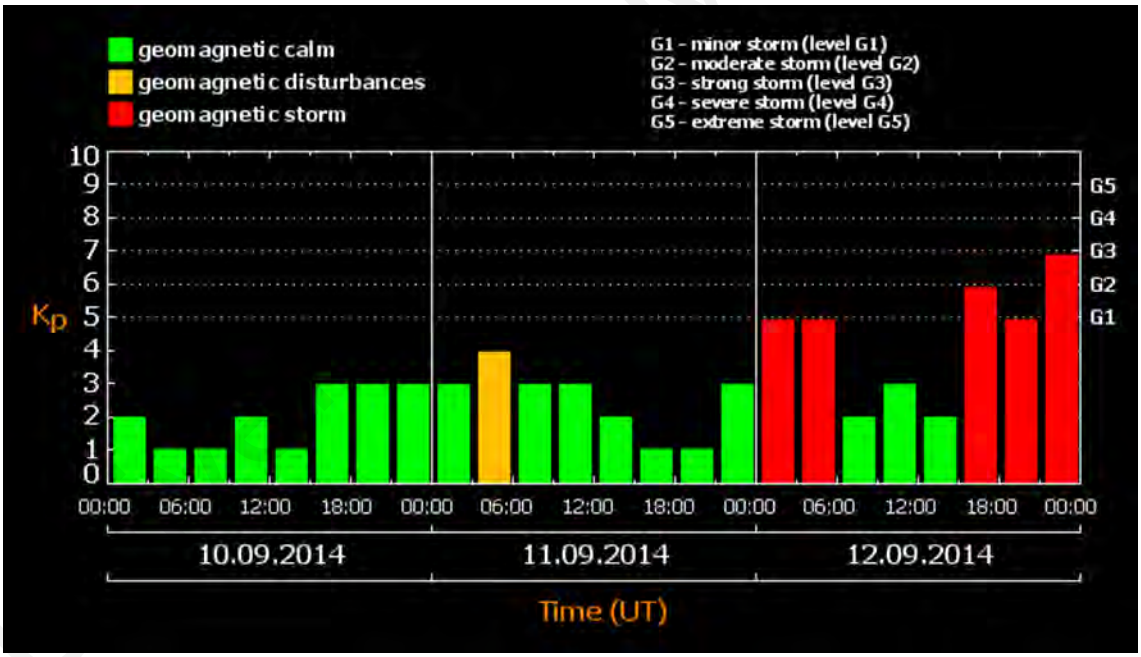

Figure 5.26: The magnetic storm level G2 (moderate) occur from 15:00 to 18:00 UT was observed.

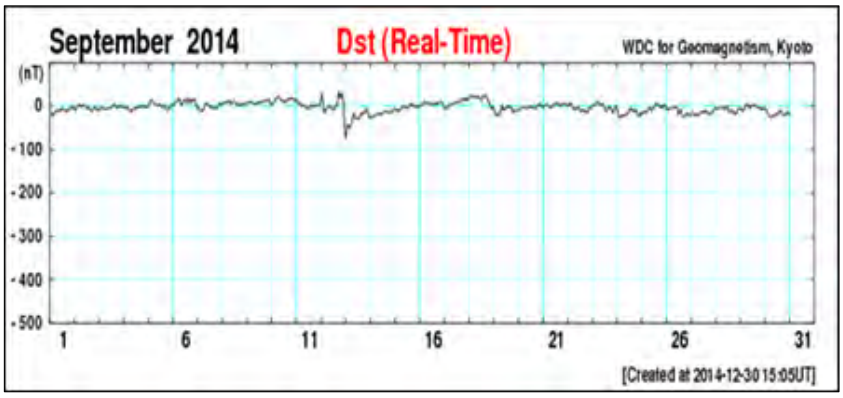

Figure 5.27: The changes in the DST (disturbance-storm time) index of geomagnetic storm on 12th September 2014.

Moreover, these events are also associated with the geomagnetic storm occurring on 12th September 2014, two days after the solar flare emission with storm level G2 (moderate). The data was recorded by magnetometer stations at Russia and Japan as shown in Figure 5.26 and Figure 5.27 respectively. The disturbance in the interplanetary medium which drives the geomagnetic storm may be due to a solar CME or high-speed stream of solar wind.

Table 5.4 shows the condition of the Sun on 10th September 2014 from the Space Weather Web Site. In brief, the proton density in solar corona is 11.7 g/cm3 with solar wind speeds exceeding 365.9 km/sec and 159 sfu radio flux. Seven Active Regions were spotted on that day with sunspot numbers 162.

Table 5.4: Parameter of the Sun during 10th September 2014.

Parameter	Value
Active Region	AR 2157 & AR2158
Solar Wind Speed	365.9 km/sec
Density	11.7protons/cm^3
X-ray Solar Flares	Class X1.6: 17:46 UT (6-hr max & 24-hr max)
The Radio Sun	10.7 cm flux: 159 sfu
Sunspot Number	162
Interplanetary Magnetic Field	B_{total}: 7.6 nT B_z: 3.4 nT north

Solar flare class X 1.6 is continuously being observed in the X-ray region for 24 hours since 1746 UT and a maximum class X 1.6 was detected on 1746 UT. The explosion of the X-class solar flare during that day came from active regions 2157 and 2158.

The probability of solar emissions is high when a large sunspot group is present, as, for this event, the number of sunspots spotted during the day is 162 with 159 SFU. The total magnetic field at the interplanetary medium is 7.6 nT and it was directed towards the north with Bz is 2.4 nT north.

5.2.8 Observation on 11th March 2015

This type IV solar radio burst was preceded and followed by type III solar radio burst. It occurred at 1615-1623 UT with weaker structure from frequency range 250-900 MHz. It was detected from BLEN7M station only. A single type III solar radio burst preceded the type IV solar radio burst at the frequency range above 10-750 MHz with weaker structure at 0000-0955 UT. Then, another type III solar radio burst followed the type IV solar radio burst a minute after that at 1624-1630 UT with storm type III solar radio burst at the frequency range 40-250 MHz as shown in Figure 5.28. In addition, a group of type III solar radio burst appeared at 1847-1850 MHz starting from 20-85 MHz.

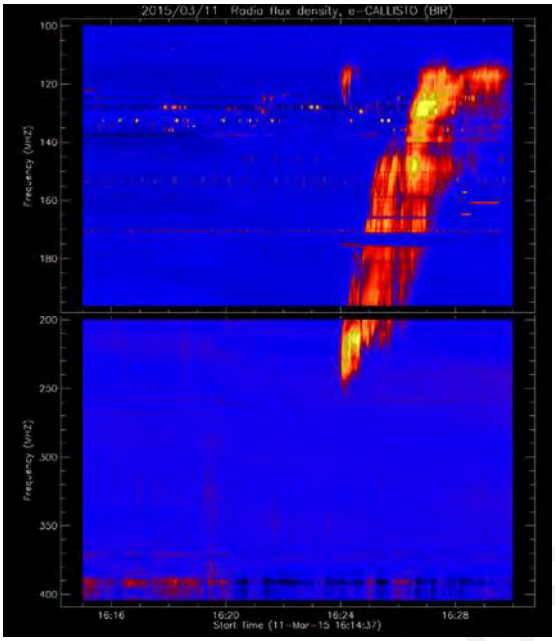

Figure 5.28: Solar radio burst type IV was followed by a storm type III burst.

During this event, a solar flare of class X 2.1 which is one of the more powerful types of solar flare was observed at 16:11:00 UT until 16:29:00 UT with the maximum peak at 16:22:00 UT. It was ejected from AR 2297 with sunspot number reported during this day is 42. Figure 5.29 demonstrates the location of sunspot AR 2297 that was located near to the East limb of the Sun and not directed towards the Earth. The solar wind velocity recorded is 376 km/s, and the density of protons is 4.0 protons/cm^3.

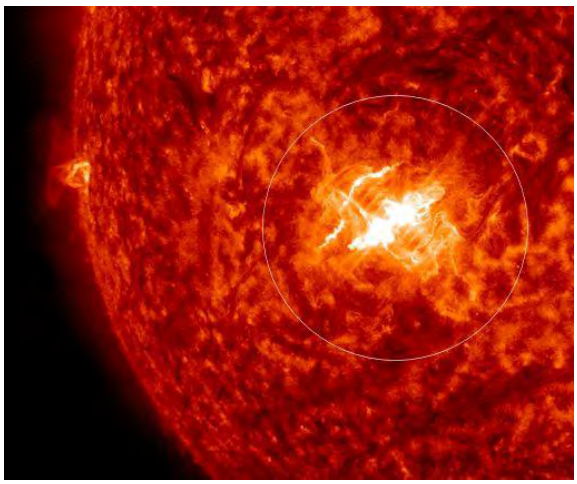

Figure 5.29: Sunspot AR 2297 on 11th March 2015 has a 'beta-gamma-delta' magnetic field that harbors energy for X-class solar flares.

In addition, a poor CME event emerged with the first appearance at 17:00:05 UT with speed of 240 km/s. It is predicted with this slow velocity, the ejected plasma will definitely not reach the Earth. Unfortunately, only geomagnetic calm was reported for these events although it was generated by the X-class flare which can impact the Earth's magnetic field. This might happen because of the thermal emission of the solar radio burst produces lower energy.

In brief, this event shows a single type III solar radio burst with weaker structure preceding the type IV solar radio burst with the duration exceeding one hour before the onset of the type IV solar radio burst. Generally, single type III solar radio burst has a small scale energy release. Thus, the energy generated by type III is insufficient in providing extra energy to the type IV solar radio burst in a producing bigger impact on the Earth's magnetic field. However, this type IV solar radio burst was followed by a nice and bright storm type III solar radio burst, but not providing any effect to the geomagnetic storm level.

In addition, the active region that was responsible in ejecting the solar events was not directed towards the Earth. The energy was then dispersed into the interplanetary medium. Furthermore, the solar wind speed during these events is too slow to produce a geomagnetic storm.

5.2.9 Observation on 24th April 2015

Figure 5.30 shows the data for type IV solar radio burst which was preceded by a weaker single and a group of type III solar radio burst. The group of type III solar radio burst occurred for four minutes and the single type III solar radio burst lasted between 0515-1850 UT at the frequency range 110-230 MHz for group of burst and 44-370 MHz for single burst. There are four type IV solar radio bursts detected from CPH, HIMAP, and RWANDA. Flare continua of type IV solar radio burst has onset at 1053-1056 UT in

the frequency range of 44-82 MHz. A 3-stationary type IV solar radio burst appeared at 0511-0515 UT, 0810-0815 UT and 1730-1736 UT with frequency range 50-900 MHz and 1120-1400MHz.

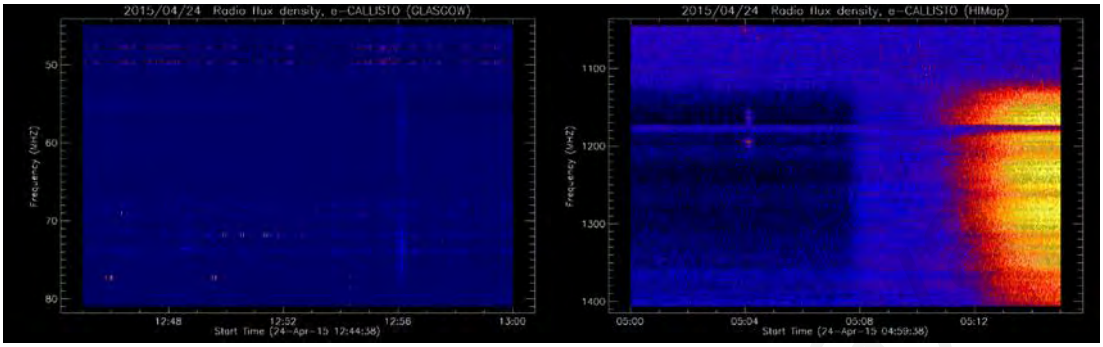

Figure 5.30: Type IV solar radio burst was preceded by weaker of single and group of type III burst solar radio burst.

As expected from these delicate events, it was only associated with solar flare C-class and geomagnetic calm. The weaker emission of solar radio burst detected on the spectrogram showed a low energy, not enough to propel it through the solar corona. In addition, as shown in Table 5.5, the solar wind velocity is slow at 367.4 km/s only. There are 9 active regions during this event which are AR 2321, AR 2324, AR 2325, AR 2326, AR 2327, AR 2330, AR 2331, AR 2332 and AR 2333.

Table 5.5: Parameter of the Sun during 24th April 2015.

Parameter	Value
Active Region	9
Solar Wind Speed	367.4 km/sec
Density	3.4 protons/cm^3
X-ray Solar Flares	Class C2: 08:43 UT (24-hr max)
The Radio Sun	10.7 cm flux: 141 sfu
Sunspot Number	110
Interplanetary Magnetic Field	B_{total}: 4.0 nT B_z: 0.8 nT north

This example of solar radio burst event was almost same with the solar radio burst event on 11th March 2015. A single and storm type III solar radio burst with frail structures occurred only a few minutes before the presence of the type IV solar radio burst. Thus, only a small amount of energy came from the type III solar radio burst. Besides, there is a slow solar wind speed with 367.4 km/s and no CME detected during this time.

Overall, by examining the characteristics and parameters of type III solar radio burst before the emission of type IV solar radio burst, it can provide the information on predict the level of geomagnetic storms.

5.2.10 Observation on 5th September 2015

The radio signatures associated with the geomagnetic event of 5th September 2015 are shown in Figure 5.31. There were three type IV solar radio bursts detected from three stations (ALMATY, BLEN5M, and MRO) with flare continua and stationary type IV solar radio burst. Flare continua occurred from the 55-165 MHz frequency range at 1155-1200 UT. A stationary type IV solar radio burst occurred during the intervals 1700-1705 UT and 0945-0952 UT. The first one was in the frequency range 990-1260 MHz and the second in the 500-700 MHz. A single type III solar radio burst was detected from three stations (ALMATY, BLENSW and HB9SCT) with 6 structure of type III solar radio burst of which four of them preceded the type IV solar radio burst at 0214 UT (50-165 MHz), 0214 UT (180-320 MHz), 0829 UT (20-50 MHz) and 0846 UT (25-65 MHz). The other two type III solar radio burst happened at 1656 UT at the frequency range 20-80 MHz and the second one at 1314 UT with the frequency range of 240-370 MHz with all having a duration of 1-3 seconds.

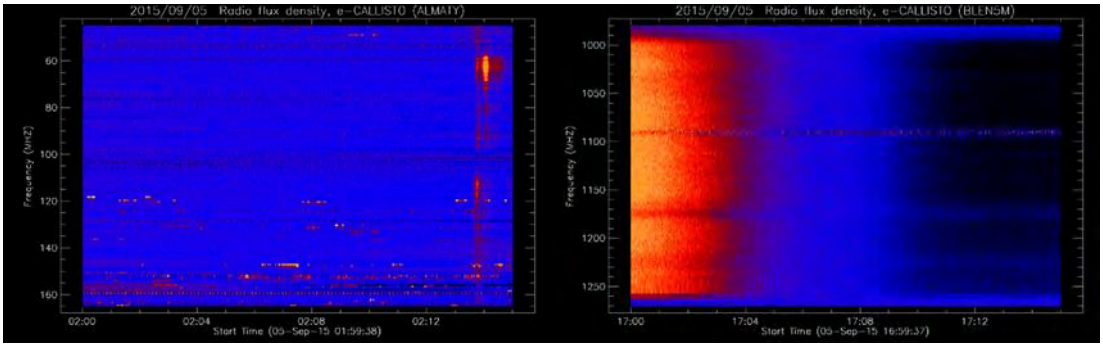

Figure 5.31: Single type III burst and continua type IV burst.

This type IV solar radio burst event was preceded by a type III solar radio burst have a moderate geomagnetic storm on 7 September 2015. Along with this event, only a B3-class flare observed. There are 5 Active Regions during this event as presented in Figure 5.32 which are AR 2411, AR 2409, AR 2410, AR 2405 and AR2406.

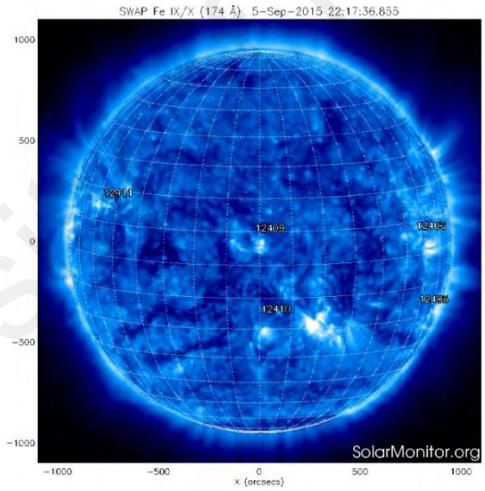

Figure 5.32: Location of sunspot that erupt in this event.

The geomagnetic storm level of minor storm (G1) and moderate storm (G2) were detected despite the powerless flare class on that day. It may be due the presence of the CME that blasted plasma towards the Earth's magnetic field. The SDO movie from SOHO shows a plasma racing away form the core of a CME but this CME is not heading directly toward the Earth. The geomagnetic storm broke out as Earth passes through a

fast-moving stream of solar wind. Other parameters that contributed to the event are presented in Table 5.6.

Table 5.6: Parameter of the Sun during 5th September 2015.

Parameter	Value
Active Region	5
Solar Wind Speed	425.5 km/sec
Density	4.3 protons/cm^3
X-ray Solar Flares	Class B3: 02:15 UT (24-hr max)
The Radio Sun	10.7 cm flux: 90 sfu
Sunspot Number	36
Interplanetary Magnetic Field	B_{total}: 6.5 nT B_z: 0.7 nT north

5.3 Effect of radio frequency interference (RFI) on solar bursts detections.

The effects of radio frequency interference (RFI) often make it difficult to estimate the exact measurement of solar radio bursts. Aware of this issue, the external RFI from terrestrial interference and man-made RFI that effect solar radio burst spectrograms was studied.

The Signal to Noise Ratio (SNR) with respect to the terrestrial interference is defined as the ratio of the power of a signal (important information) and the power of background noise (unwanted signal):

$$SNR = \frac{P_{signal}}{P_{noise}} \tag{5.1}$$

SNR values are calculated by taking one peak at spectrogram (eg: 800 MHz) and sliding the cursor along the chosen frequency for an average of the power signal and power noise. Figure 5.33 shows an example of the RAPP software to calculate the SNR values. The RAPP software can be freely downloaded from the e-Calisto website and is user friendly. The first step before opening the file, the setup of the software should be

done by choosing standard II from color scales and keeping the colorscale, and automatic background subtraction from the options bar. The power values can be obtained from the bottom right of the box (shown in the red circle).

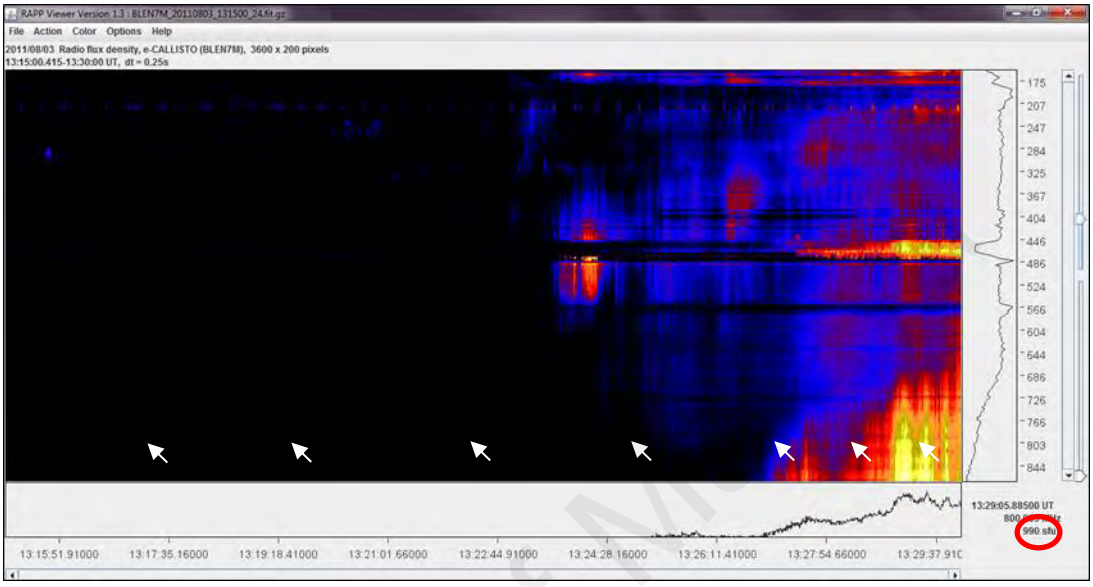

Figure 5.33: RAPP software CALLISTO to calculate the SNR value.

The average percentages of the SNR with respect to the terrestrial interference over the solar signal are calculated in Table 5.7. It was calculated based on the RFI that affects the spectrogram of the type III solar radio burst and type IV solar radio burst from various stations. It has been clearly shown that different types of RFI have influenced the level of detection of this solar radio burst. The percentages of SNR for 13th December 2006 (type III), 3rd August 2011 (type IV) and 7th March 2012 (type IV) are slightly higher compared with others of 2.723 (type III), 3.472 (type IV) and 2.186 (type IV) respectively.

Table 5.7: SNR of solar radio burst.

Date	Solar Burst SNR	
	Type III	Type IV
13th December 2006	2.723	1.542
3rd November 2008	1.122	1.429
1st August 2010	1.175	1.349
3rd August 2011	1.045	3.472
7th March 2012	1.024	2.186
15th March 2013	1.125	1.010
10th September 2014	1.055	1.059
11th March 2015	1.152	1.071
24th April 2015	1.027	1.026
5th September 2015	1.059	1.061

The study by (Abidin et al., 2015) found that the RFI severely affects CALLISTO within radio astronomical windows below 870 MHz (in the ranges of 80-110 MHz 460-500 MHz). They also found that all stations are relatively free from RFI at 270-290 MHz. Thus, this study validates the suggestion that most of the RFI severely affects CALLISTO and free in the given range. As can be seen from Figure 5.4 (both type), Figure 5.7 (type III), Figure 5.8 (both type), Figure 5.11 (type IV), Figure 5.14 (type III), Figure 5.18 (both type), Figure 5.22 (type IV), Figure 5.30 (type IV) and Figure 5.31 (both type), it was found that the RFI affects the solar radio burst emission from 450-500 MHz, 60-110 MHz, 260-265 MHz, 1090-1095 MHz and 1270-1280 MHz.

Therefore, it is important to refer to the spectrum allocation designated by countries that host the stations to find the sources of RFI that affect the solar radio bursts observatories. Table 5.8 presents the spectrum allocation of each country where the solar radio bursts was obtained, along with the sources of the RFI at certain frequency.

Table 5.8: Spectrum allocation by their country.

Station	Frequency (MHz)	Source
SSRT, Russia	60-80	Fixed Mobile and Broadcasting, Fixed Mobile, Aeronautical Radio navigation.
MRT, Mauritius	90-100	Broadcasting, FM Sound Broadcasting
ALMATY, Kazakhstan	100-110	Broadcasting, Aeronautical Radio navigation
BIR, Ireland	170-175	Fixed Mobile, Fixed Mobile Broadcasting
KRIM, Ukraine	260-265	Fixed Mobile
SSRT, Russia	460-480	Fixed Mobile, Meteorological-Satellite (Space-To-Earth), Fixed Mobile Broadcasting
MRT, Mauritius	450-500	Fixed Mobile, Meteorological-Satellite (Space-To-Earth), Tv Broadcasting
BLEN7M, Switzerland	460-490	Mobile, Broadcasting Land Mobile, Broadcasting Primary. Land Mobile Secondary.
	470-480	
	480-490	
BLEN5M, Switzerland	1090-1095	Aeronautical Radio navigation
HIMap, Switzerland	1270-1280	Radio navigation Earth Exploration-Satellite (Active) Radiolocation Radio Navigation-Satellite (Space-To-Earth) (Space-To space) Space Research (Active)

The main origin of the RFI affected the spectrogram are generally due to Fixed Mobile and Broadcasting, Fixed Mobile, Aeronautical Radio navigation, Broadcasting, FM Sound Broadcasting, Meteorological-Satellite (Space-To-Earth), Tv Broadcasting, Mobile, Broadcasting Land Mobile, Broadcasting Primary, Land Mobile Secondary, Radio navigation Earth Exploration-Satellite (Active) Radiolocation Radio Navigation-Satellite (Space-To-Earth) (Space-To space) Space Research (Active). In addition, it

clearly shows most of the CALLISTO stations are contaminated by fixed mobile broadcasting signals. The result of this study indicates that only a small percentage of RFI disturbs the solar radio burst, either by external RFI from terrestrial interference or man-made RFI. Thus, it validates the suggestion that the RFI mostly severely affects CALLISTO from 80-110 MHz and 460-500 MHz and is relatively free from RFI at 270-290 MHz.

The spectrum allocation for the Switzerland were provided by Swiss National Frequency Allocation Plan and Specific Assignments, Mauritius by Mauritius Frequency Allocations Table 2013 (MFAT 2013), while for Russia, Ukraine, Ireland and Kazakhstan from National Radio Frequency Allocation Table 2016.

CHAPTER 6: CONCLUSIONS

In summary, it has been shown that it is possible to use the CALLISTO spectrometer to obtain solar radio burst data. The spectrogram provided by CALLISTO has a good quality and clear characteristics of solar radio burst emission. From the data obtained, the significance is that both types III and IV solar radio burst shows a strong relation to the solar activity. Hence, there is no doubt that the CALLISTO Spectrometer is such a great tool for observing solar radio burst emission.

The findings of this study suggest that the statistical data shows most of the type IV solar radio bursts were preceded by type III solar radio bursts rather than other types of solar radio bursts. From 37 events of type IV solar radio bursts, 54% of type III solar radio bursts emission occur in conjunction with the type IV solar radio bursts emission and the rest with other types and no bursts were detected. In addition, it was found in the event of the type III solar radio burst occurring before the type IV solar radio burst, the association of geomagnetic storm was greater compared to the type IV solar radio burst event alone. With 20 events of type IV solar radio burst being preceded by type III solar radio burst, there are 5 events associated with great geomagnetic storms from 6 to 8 k_p index. While, for type IV solar radio burst alone without the associated type III solar radio burst, 5 events were associated with geomagnetic storm from 5 to 8 k_p index, with three of them at 5 k_p index. Even though type IV solar radio burst alone also have geomagnetic storm, but it occurs only at the index of 5 and only two events at 7 and 8 k_p index, compared to the type IV solar radio burst that have been preceded by type III solar radio burst where it associated with 6 to 8 k_p index which is registered as a large one.

In brief, it has been shown that type IV solar radio bursts have a high probability of being followed by a geomagnetic disturbance. The occurrence of type IV solar radio bursts alone (without type III solar radio burst) is not enough, since the corresponding

solar plasma cloud behind the shock front has a weaker particle density to cause an observable geomagnetic effect. Similarly, the occurrence of a type III solar radio bursts without type IV solar radio burst may not be sufficient to influence the geomagnetic activity, since it has no shock front associated with it. This association between type III and type IV solar radio burst can be explained by the fact that both of these solar radio bursts are generated by fast electrons. The disturbance which gives rise to type III solar radio bursts have high velocities and may be either an electron stream or transverse shock. While, the electrons which give rise to type IV solar radio bursts are principally have a similar velocity range.

Other than that, it was shown that some events which are not preceded by a type III solar radio burst has a high geomagnetic storm index, this might be due to the possibility of the solar magnetic field being ejected by the CME and/or the speed of the solar wind. Otherwise, this study has found that although the events have a great solar flare, the level of the magnetic disturbance is still low. This might be due to several factors. The high energy from the solar flare may be ejected from the active region that is not directed towards the Earth, thus only a small amount of energy disturbs the Earth's magnetic field.

Thus, it can be concluded that the structure of the type III and type IV solar radio burst shows a good relationship with solar activity. Its characteristic gives information about the particle ejected from the solar surface, thus providing valuable information. After all, the sequence of type III solar radio burst occurs before the formation of type IV solar radio bursts is determined by the positions of the associated flares in the solar longitude.

For good measure, it was found that only a small percentage of RFI disturbs the solar radio burst that have been used in this study. It was affected by the external RFI either from terrestrial interference or man-made RFI.

Overall, by studying the effect of solar events on space and ground-based technology, the findings of this study will help by providing information as a first line of defense to our technology. Estimating the level of the geomagnetic storm by analyzing the characteristics of solar radio burst provides extra time because geomagnetic storm arrives at the Earth's magnetic fields several days after the commencement of solar events.

REFERENCES

Abidin, Z. Z., Anim, N. M., Hamidi, Z. S., Monstein, C., Ibrahim, Z. A., Umar, R., . . . Sukma, I. (2015). Radio frequency interference in solar monitoring using CALLISTO. *New Astronomy Reviews, 67*, 18-33.

Ali, M., Sabri, S., Hamidi, Z., Husien, N., Shariff, N., Zainol, N., . . . Monstein, C. (2016). *e-CALLISTO network system and the observation of structure of solar radio burst Type III.* Paper presented at the Industrial Engineering, Management Science and Application (ICIMSA), 23-26 May 2016, Jeju Island, Korea.

Antalová, A. (1967). The photospheric situation connected with the development of flares accompanied by the type IV radio bursts. *Bulletin of the Astronomical Institutes of Czechoslovakia, 18*, 61.

Bak, P. (1993). Self-organized criticality in astrophysics. *In Cellular Automata,* 281-293.

Balogh, A., Lanzerotti, L. J., & Suess, S. T. (2007). *The heliosphere through the solar activity cycle.* Chichester, UK: Springer Science & Business Media.

Bell, B. (1963a). Solar radio bursts of spectral types II and IV: their relations to optical phenomena and to geomagnetic activity. *Smithsonian Contributions to Astrophysics, 5*, 239-257.

Bell, B. (1963b). Type IV solar radio bursts, geomagnetic storms, and polar cap absorption (PCA) events. *Smithsonian Contributions to Astrophysics, 8*, 119.

Benz, A. O., & Saint-Hilaire, P. (2003). Solar flare electron acceleration: Comparing theories and observations. *Advances in Space Research, 32*(12), 2415-2423.

Bhattacharya, A., Roy, K., Pandit, J., & Nag, A. (2013). Automated PC-based control and monitoring of Radio observations using LPDA. *Procedia Technology, 10*, 348-355.

Bohm, D., & Gross, E. P. (1949). Theory of plasma oscillations. A. Origin of medium-like behavior. *Physical Review, 75*(12), 1851.

Bonnet, R. M. (2004). Recent Progress and future prospects in solar physics, and their relevance for planet earth. *Surveys in Geophysics, 25*(5-6), 371-440.

Bougeret, J.-L., Fainberg, J., & Stone, R. (1984). Interplanetary radio storms. I-Extension of solar active regions through the interplanetary medium. *Astronomy and Astrophysics, 136*, 255-262.

Burkhardt, G., Esser, U., Hefele, H., Heinrich, I., Hofmann, W., Matas, V., . . . Zech, G. (1998). Planetary System *Literature 1997, Part 1* (pp. 589-747). Berlin, Heidelberg: Springer.

Cairns, I. H., Robinson, P., & Zank, G. (2000). Progress on coronal, interplanetary, foreshock, and outer heliospheric radio emissions. *Publications of the Astronomical Society of Australia, 17*(1), 22-34.

Campos Rozo, J., & Vargas Dominguez, S. (2014). SunPy: Python for Solar Physics. An implementation for local correlation tracking. *Srednjeeuropski Astrofizički Bilten, 38*(1), 67-72.

Cane, H., & Reames, D. (1988). Some statistics of solar radio bursts of spectral types II and IV. *The Astrophysical Journal, 325*, 901-904.

Cane, H. V., Erickson, W., & Prestage, N. (2002). Solar flares, type III radio bursts, coronal mass ejections, and energetic particles. *Journal of Geophysical Research: Space Physics, 107*(A10).

Chaisson, E., & McMillan, S. (2014). Astronomy Today, Global Edition.

Cho, K.-S., Lee, J., Gary, D., Moon, Y.-J., & Park, Y. (2007). Magnetic field strength in the solar corona from type II band splitting. *The Astrophysical Journal, 665*(1), 799.

Christe, S., Krucker, S., Glesener, L., Shih, A., Saint-Hilaire, P., Caspi, A., ... & Dennis, B. (2017). Exploring impulsive solar magnetic energy release and particle acceleration with focused hard X-ray imaging spectroscopy. *arXiv preprint arXiv:1701.00792*.

Christiansen, W., Mathewson, D., Pawsey, J., Smerd, S., Boischot, A., Denisse, J., . . . Firor, J. (1960). *A study of a solar active region using combined optical and radio techniques.* Paper presented at the Annales d'Astrophysique.

Ellingson, S. W. (2005). *Spectral occupancy at VHF: implications for frequency-agile cognitive radios.* Paper presented at the Vehicular Technology Conference, 2005. VTC-2005-Fall. 2005 IEEE 62nd, Dallas, TX, USA.

Fokker, A. (1963). Type IV solar radio emission. *Space Science Reviews, 2*(1), 70-90.

Gary, D. E., & Keller, C. U. (2004). *Solar and space weather radiophysics: current status and future developments* (Vol. 314). Netherlands: Springer Science & Business Media.

Ginzburg, V., & Zhelezniakov, V. (1958). On the possible mechanisms of sporadic solar radio emission (radiation in an isotropic plasma). *Astronomicheskii Zhurnal, 35*, 694.

Gopalswamy, N. (2016). *Low-frequency radio bursts and space weather*. Paper presented at the URSI Asia-Pacific Radio Science Conference (URSI AP-RASC), 21-25 August 2016, Seoul, Korea.

Goss, W. (2013). A Brief, Basic Guide to Terms and Concepts of Solar Radio Astronomy *Making Waves* (pp. 13-42). Verlag, Berlin, Heidelberg: Springer.

Gurnett, D., Hospodarsky, G., Kurth, W., Williams, D., & Bolton, S. (1993). Fine structure of Langmuir waves produced by a solar electron event. *Journal of Geophysical Research: Space Physics, 98*(A4), 5631-5637.

Gurnett, D. A. (1995). Heliospheric radio emissions. *Space Science Reviews, 72*(1-2), 243-254.

Hamidi, Z., Abidin, Z., Ibrahim, Z., Monstein, C., Shariff, N., & Sabaghi, M. (2012). The Beginning Impulsive of Solar Burst Type IV Radio Emission Detection Associated with M Type Solar Flare. *International Journal of Fundamental Physical Sciences, 2*(2), 29-31.

Hamidi, Z., Ibrahim, M., Shariff, N., & Monstein, C. (2014). A case study of explosion a single solar burst type III and IV due to active region AR1890. *International Letters of Chemistry, Physics and Astronomy, 19*(2), 171-180.

Hamidi, Z., Monstein, C., & Shariff, N. (2014). Radio Observation of Coronal Mass Ejections (CMEs) Due to Flare Related Phenomenon on 7th March 2012. *International Letters of Chemistry, Physics and Astronomy, 11*(3), 243-256.

Hamidi, Z., Shariff, N., & Monstein, C. (2012). High Time Resolution Observation of Solar Radio of A Group Type III And U Burst Associated of Solar Flares Event. *The International Journal of Engineering and Science, 1*(1), 101-103.

Hamidi, Z., Zainol, N., Ali, M., Sabri, S., Shariff, N., Faid, M., . . . Monstein, C. (2016). *Signal detection of the solar radio burst type III based on the CALLISTO system project management.* Paper presented at the Industrial Engineering, Management Science and Application (ICIMSA), 23-26 May 2016, Jeju Island, Korea.

Hamidi, Z. S. (2014). Probability of Solar Flares Turn Out to Form a Coronal Mass Ejections Events Due to the Characterization of Solar Radio Burst Type II and III. *International Letters of Chemistry, Physics and Astronomy, 16*, 1-85 .

Hamidi, Z. S., Sabri, S., Shariff, N., & Monstein, C. (2015). The Evolution of Unstable'Beta-Gamma'Magnetic Fields of Active Region AR 2222. *International Letters of Chemistry, Physics and Astronomy, 48*, 95-102.

Higgins, P. A. (2012). *Sunspot Group Evolution and the Global Magnetic Field of the Sun.* Trinity College Dublin.

Kocz, J., Briggs, F., & Reynolds, J. (2010). Radio frequency interference removal through the application of spatial filtering techniques on the parkes multibeam receiver. *The Astronomical Journal, 140*(6), 2086.

Kong, X.-L., Chen, Y., Li, G., Feng, S.-W., Song, H.-Q., Guo, F., & Jiao, F.-R. (2012). A broken solar type II radio burst induced by a coronal shock propagating across the streamer boundary. *The Astrophysical Journal, 750*(2), 158.

Kumar, P., Bhatt, Y. C., Jain, R., & Shishodia, Y. S. (2015). Solar flare and its interaction with the Earth atmosphere: An Introduction. *Physics Education, 31*(2), 6.

Kumar, P., & Manoharan, P. (2013). Eruption of a plasma blob, associated M-class flare, and large-scale extreme-ultraviolet wave observed by SDO. *Astronomy & Astrophysics, 553*, A109.

Kundu, M. (1962). Association of centimeter-wave bursts with different spectral types of meter-wave bursts of solar radio emission. *Journal of Geophysical Research, 67*(7), 2695-2706.

Kundu, M. R. (1965). *Solar radio astronomy*. New York; London: Interscience Publishers.

Landscheidt, T. (1984). Cycles of solar flares and weather *Climatic Changes on a Yearly to Millennial Basis* (pp. 473-481): Springer.

Lang, K. R. (2009). Our Violent Sun. *The Sun from Space* (pp. 253-336). Berlin,Heidelberg: Springer.

Li, B., Cairns, I. H., & Robinson, P. A. (2008). Simulations of coronal type III solar radio bursts: 2. Dynamic spectrum for typical parameters. *Journal of Geophysical Research: Space Physics, 113*(A6).

Lin, R., Potter, D., Gurnett, D., & Scarf, F. (1981). Energetic electrons and plasma waves associated with a solar type III radio burst. *The Astrophysical Journal, 251*, 364-373.

Mazar, H. (2009). *An analysis of regulatory frameworks for wireless communications, societal concerns and risk: The case of Radio Frequency (RF) allocation and licensing*. Florida, USA: Universal-Publishers.

McLean, D. (1959). Solar radio emission of spectral type IV and its association with geomagnetic storms. *Australian Journal of Physics, 12*(4), 404-417.

Melnik, V., Konovalenko, A., Rucker, H., Boiko, A., Dorovskyy, V., Abranin, E., & Lecacheux, A. (2011). Observations of powerful type III bursts in the frequency range 10–30 MHz. *Solar Physics, 269*(2), 335-350.

Monstein, C (2015). Catalog of dynamic electromagnetic spectra. *Physics, Astronomy and Electronics Work Bench,* 1-16.

Moreton, G. E. (1964). The association of bremsstrahlung X rays with explosive flares. *NASA Special Publication, 50*, 209.

Mumford, S. J., Christe, S., Pérez-Suárez, D., Ireland, J., Shih, A. Y., Inglis, A. R., . . . Hughitt, K. (2015). SunPy—Python for solar physics. *Computational Science & Discovery, 8*(1), 014009.

Narukage, N., Eto, S., Kadota, M., Kitai, R., Kurokawa, H., & Shibata, K. (2004). Moreton waves observed at Hida Observatory. *Proceedings of the International Astronomical Union, 2004*(IAUS223), 367-370.

NASA Goddard Space Flight Center. (2012). *Solar eruptive events*. Greenbelt, MD, United States: Holman, G. D.

Nelson, G. (1977). Three frequency observations of a moving type IV burst at the limb. *Publications of the Astronomical Society of Australia, 3*(2), 159-162.

Nelson, G., & Melrose, D. (1985). Type II bursts. *Solar Radiophysics: Studies of Emission from the Sun at Metre Wavelengths*, 333-359.

Nindos, A., Aurass, H., Klein, K.-L., & Trottet, G. (2008). Radio emission of flares and coronal mass ejections. *Solar Physics, 253*(1-2), 3.

Pick, M., & Vilmer, N. (2008). Sixty-five years of solar radioastronomy: flares, coronal mass ejections and Sun–Earth connection. *The Astronomy and Astrophysics Review, 16*(1-2), 1-153.

Porko, J.-P. G. (2011). *Radio frequency interference in radio astronomy* (Master's thesis). Retrieved from https://aaltodoc.aalto.fi/handle/123456789/3739

Ramli, N., Hamidi, Z., Abidin, Z., & Shahar, S. (2015). *The relation between solar radio burst types II, III and IV due to solar activities.* Paper presented at the International Conference on Space Science and Communication (IconSpace), 10-12 August 2015, Langkawi, Malaysia.

Rathore, B. S., Gupta, D. C., & Parashar, K. (2014). Relation between Solar Wind Parameter and Geomagnetic Storm Condition during Cycle-23. *International Journal of Geosciences, 5*(13), 1602.

Reiner, M., Vourlidas, A., Cyr, O. S., Burkepile, J., Howard, R., Kaiser, M., . . . Bougeret, J.-L. (2003). Constraints on coronal mass ejection dynamics from simultaneous radio and white-light observations. *The Astrophysical Journal, 590*(1), 533.

Richardson, I., Webb, D., Zhang, J., Berdichevsky, D., Biesecker, D., Kasper, J., . . . Wu, C. C. (2006). Major geomagnetic storms (Dst≤− 100 nT) generated by corotating interaction regions. *Journal of Geophysical Research: Space Physics, 111*(A7), 1-17.

Sakurai, K. (1973). The initial stage of development of type IV radio bursts and the relation to expanding magnetic bottles. *Solar Physics, 31*(2), 483-492.

Schmidt, J., Cairns, I. H., & Hillan, D. (2013). Prediction of type II solar radio bursts by three-dimensional MHD coronal mass ejection and kinetic radio emission simulations. *The Astrophysical Journal Letters, 773*(2), L30.

Thejappa, G., MacDowall, R., & Bergamo, M. (2012). Emission Patterns of Solar Type III Radio Bursts: Stereoscopic Observations. *The Astrophysical Journal, 745*(2), 187.

Thejappa, G., MacDowall, R., Bergamo, M., & Papadopoulos, K. (2012). Evidence for the oscillating two stream instability and spatial collapse of Langmuir waves in a solar type III radio burst. *The Astrophysical Journal Letters, 747*(1), L1.

Thompson, A. (1962). Type IV (continuum) radio bursts from the sun. *Journal of the Physical Society of Japan Supplement, 17*, 198.

Umar, R., Abidin, Z. Z., Ibrahim, Z. A., Rosli, Z., & Noorazlan, N. (2014). Selection of radio astronomical observation sites and its dependence on human generated RFI. *Research in Astronomy and Astrophysics, 14*(2), 241.

Vršnak, B., Aurass, H., Magdalenić, J., & Gopalswamy, N. (2001). Band-splitting of coronal and interplanetary type II bursts-I. Basic properties. *Astronomy & Astrophysics, 377*(1), 321-329.

Vršnak, B., Magdalenić, J., Aurass, H., & Mann, G. (2002). Band-splitting of coronal and interplanetary type II bursts-II. Coronal magnetic field and Alfvén velocity. *Astronomy & Astrophysics, 396*(2), 673-682.

Vršnak, B., Magdalenić, J., & Zlobec, P. (2004). Band-splitting of coronal and interplanetary type II bursts-III. Physical conditions in the upper corona and interplanetary space. *Astronomy & Astrophysics, 413*(2), 753-763.

White, S. M. (2007). Solar radio bursts and space weather. *Asian Journal of Physics, 16*, 189-207.

Wild, J. (1950). Observations of the spectrum of high-intensity solar radiation at metre wavelengths. III. Isolated bursts. *Australian Journal of Chemistry, 3*(4), 541-557.

Wild, J. P., Sheridan, K., & Neylan, A. (1959). An investigation of the speed of the solar disturbances responsible for Type III radio bursts. *Australian Journal of Physics, 12*(4), 369-398.

Yoon, P. H. (1997). Plasma emission by a nonlinear beam instability in a weakly magnetized plasma. *Physics of Plasmas, 4*(11), 3863-3881.

Zlotnik, E., Zaitsev, V., Aurass, H., & Mann, G. (2005). What can we learn about accelerated electrons in coronal loops from analysis of solar type IV radio bursts? *Advances in Space Research, 35*(10), 1774-1777.

Zucca, P., Carley, E., McCauley, J., Gallagher, P., Monstein, C., & McAteer, R. (2012). Observations of low frequency solar radio bursts from the Rosse solar-terrestrial observatory. *Solar Physics, 280*(2), 591-602.

LIST OF PUBLICATIONS AND PAPERS PRESENTED

LIST OF PUBLICATION

Abidin, Z. Z., Anim, N. M., Hamidi, Z. S., Monstein, C., Ibrahim, Z. A., **Ramli, N**., . Sukma, I. (2015). Radio frequency interference in solar monitoring using CALLISTO. *New Astronomy Reviews, 67*, 18-33.

LIST OF PAPERS PRESENTED

Ramli, N., Hamidi, Z., Abidin, Z., & Shahar, S. (2015). *The relation between solar radio burst types II, III and IV due to solar activities.* Paper presented at the International Conference on Space Science and Communication (IconSpace), 10-12 August 2015, Langkawi, Malaysia.

Hamid, Z. S., Shariff, N. N. M., Ibrahim, Z. A., & **Ramli, N**. (2015). Investigation of the statistical properties of solar radio burst type II and III. Paper presented at the International Conference on Space Science and Communication (IconSpace), 10-12 August 2015, Langkawi, Malaysia.

APPENDIX A - CODING OF SUNPY FOR DATA ANALYSIS

```
%%%%EXAMPLE FROM LOCAL FOLDER

from matplotlib import pyplot as plt
from matplotlib import cm
import sunpy
from sunpy.spectra.sources.callisto import CallistoSpectrogram
image = CallistoSpectrogram.read("M:\MyPython\BLEN7M_20120813_123000_24.fit.gz ")
image = image.linearize_freqs(1)
nobg = image.subtract_bg()
nobg.plot(cmap=cm.gist_ncar,vmin=5)# cm.hot, cm.spectral, cm.gist_ncar, cm.jet
plt.ylabel("Frequency [MHz]")
plt.xlabel("Time [UT]")
plt.title("Bleien Switzerland")
plt.show()
```